THE JOURNAL OF BIOLOGICAL CHEMISTRY
Vol. 280, No. 14, Issue of April 8, pp. 14028–14041, 2005
Printed in U.S.A.

Group VIB Ca^{2+}-independent Phospholipase $A_2\gamma$ Promotes Cellular Membrane Hydrolysis and Prostaglandin Production in a Manner Distinct from Other Intracellular Phospholipases A_2*

Received for publication, December 7, 2004, and in revised form, January 14, 2005
Published, JBC Papers in Press, February 4, 2005, DOI 10.1074/jbc.M413766200

Makoto Murakami‡§¶, Seiko Masuda‡§, Kaori Ueda-Semmyo‡§, Emiko Yoda‡§, Hiroshi Kuwata‡§, Yasukazu Takanezawa‡§, Junken Aoki‡§, Hiroyuki Arai‡§, Hideki Sumimoto‖, Yukio Ishikawa, Toshiharu Ishii**, Yoshihito Nakatani‡§, and Ichiro Kudo‡§**

*From the ‡Department of Health Chemistry, School of Pharmaceutical Sciences, Showa University, 1-5-8 Hatanodai, Shinagawa-ku, Tokyo 142-8555, Japan, the §Graduate School of Pharmaceutical Sciences, University of Tokyo, 7-3-1 Hongo, Tokyo 113-0033, Japan, the ‖Department of Molecular and Structural Biology, Kyushu University Graduate School of Medical Science, 3-1-1 Maidashi, Higashi-ku, Fukuoka 812-8582, Japan, and the **Department of Pathology, Toho University School of Medicine, 5-21-16 Omori-Nishi, Ohta-ku, Tokyo 143-8540, Japan*

Although group VIA Ca^{2+}-independent phospholipase $A_2\beta$ ($iPLA_2\beta$) has been implicated in various cellular events, the functions of other $iPLA_2$ isozymes remain largely elusive. In this study, we examined the cellular functions of group VIB $iPLA_2\gamma$. Lentiviral transfection of $iPLA_2\gamma$ into HEK293 cells resulted in marked increases in spontaneous, stimulus-coupled, and cell death-associated release of arachidonic acid (AA), which was converted to prostaglandin E_2 with preferred cyclooxygenase (COX)-1 coupling. Conversely, treatment of HEK293 cells with $iPLA_2\gamma$ small interfering RNA significantly reduced AA release, indicating the participation of endogenous $iPLA_2\gamma$. $iPLA_2\gamma$ protein appeared in multiple sizes according to cell types, and a 63-kDa form was localized mainly in peroxisomes. Electrospray ionization mass spectrometry of cellular phospholipids revealed that $iPLA_2\gamma$ and other intracellular PLA_2 enzymes acted on different phospholipid subclasses. Transfection of $iPLA_2\gamma$ into HCA-7 cells also led to increased AA release and prostaglandin E_2 synthesis via both COX-1 and COX-2, with a concomitant increase in cell growth. Immunohistochemistry of human colorectal cancer tissues showed elevated expression of $iPLA_2\gamma$ in adenocarcinoma cells. These results collectively suggest distinct roles for $iPLA_2\beta$ and $iPLA_2\gamma$ in cellular homeostasis and signaling, a functional link between peroxisomal AA release and eicosanoid generation, and a potential contribution of $iPLA_2\gamma$ to tumorigenesis.

Phospholipase A_2 (PLA_2)[1] catalyzes the hydrolysis of the *sn*-2 position of membrane glycerophospholipids to yield free fatty acids, including arachidonic acid (AA), and lysophospholipids. Mammalian PLA_2 enzymes have been classified into four major families, including secretory PLA_2, cytosolic PLA_2 ($cPLA_2$), Ca^{2+}-independent PLA_2 ($iPLA_2$), and platelet-activating factor acetyl hydrolases, each of which occurs as multiple isoforms (1, 2). Of these, the group IV $cPLA_2$ and group VI $iPLA_2$ families represent intracellular enzymes with a catalytic serine in their lipase consensus motif. Of the $cPLA_2$ family, $cPLA_2\alpha$, $cPLA_2\beta$, and $cPLA_2\delta$ possess a Ca^{2+}-regulated C2 domain near the N terminus, and their function is Ca^{2+}-dependent, whereas $cPLA_2\gamma$ is Ca^{2+}-independent and membrane-bound (3–6). The regulatory roles for $cPLA_2\alpha$ in production of lipid mediators, including prostaglandins and leukotrienes, have been well documented in many studies, including gene targeting (7–10).

Of the emerging $iPLA_2$ family, group VIA $iPLA_2\beta$ has been implicated in various cellular events such as the basal fatty acid reacylation reaction (membrane remodeling) (11, 12), agonist-stimulated AA release and eicosanoid generation (13–16), cell proliferation (17), apoptosis (18–21), exocytosis (22, 23), vascular relaxation (24), adipogenesis (25), and activation of store-operated channels and capacitative Ca^{2+} influx (26). In $iPLA_2\beta$ transgenic mice, the enzyme is activated during myocardial infarction and causes malignant ventricular arrhythmias (27), whereas $iPLA_2\beta$ knockout mice exhibit abnormality in the motility and function of spermatozoa (28). Although $iPLA_2\beta$ is principally a cytosolic enzyme, after cell activation, it can reportedly move to the nuclear or plasma membrane in a manner dependent upon protein kinase C according to the experimental system employed (19, 29, 30). During apoptosis, caspase-3-mediated cleavage of $iPLA_2\beta$ leads to its activation (18–21), which may be functionally associated with nuclear shrinkage in apoptotic cells (19) or to recruitment of phagocytes through the release of chemoattractant lysophosphatidylcholine from apoptotic cells (21).

The second mammalian $iPLA_2$ isoform, group VIB $iPLA_2\gamma$, is homologous to $iPLA_2\beta$ in the catalytic region, whereas the N-terminal regions of these two enzymes show no similarity (31, 32). This suggests that the regulatory functions (and their underlying mechanisms) of $iPLA_2\gamma$ are distinct from those of $iPLA_2\beta$. Although some unique features of $iPLA_2\gamma$ have been recently reported, such as stable association with membranes and utilization of distinct translation initiation sites producing different sizes of enzyme (31–33), its cellular functions remain largely unknown. More recently, novel members of the $iPLA_2$ family, including $iPLA_2\delta$, which displays lysophospholipase ac-

* This work was supported by grants-in-aid for scientific research from the Ministry of Education, Science, Culture, Sports, and Technology of Japan. The costs of publication of this article were defrayed in part by the payment of page charges. This article must therefore be hereby marked "*advertisement*" in accordance with 18 U.S.C. Section 1734 solely to indicate this fact.

¶ To whom correspondence should be addressed: Dept. of Health Chemistry, School of Pharmaceutical Sciences, Showa University, 1-5-8 Hatanodai, Shinagawa-ku, Tokyo 142-8555, Japan. Tel.: 81-3-3794-8197; Fax: 81-3-3784-8245; E-mail: mako@pharm.showa-u.ac.jp.

[1] The abbreviations used are: PLA_2, phospholipase A_2; AA, arachidonic acid; $cPLA_2$, cytosolic phospholipase A_2; $iPLA_2$, Ca^{2+}-independent phospholipase A_2; BEL, bromoenol lactone; PG, prostaglandin; COX, cyclooxygenase; FCS, fetal calf serum; PBS, phosphate-buffered saline; siRNA, small interfering RNA; LA, linoleic acid; PE, phosphatidylethanolamine; PC, phosphatidylcholine; OA, oleic acid; IL-1β, interleukin-1β; ESI/MS, electrospray ionization mass spectrometry; PI, phosphatidylinositol.

tivity rather than PLA_2 activity (34), and iPLA$_2\epsilon$, iPLA$_2\zeta$, and iPLA$_2\eta$, which exhibit triacylglycerol lipase and transacylase activities (35), have been identified. Because bromoenol lactone (BEL), an $iPLA_2$ inhibitor that has been used frequently for analysis of the cellular functions of iPLA$_2\beta$, inhibits all $iPLA_2$ isozymes (31, 34, 35), some of the functions of iPLA$_2\beta$ previously described only on the basis of inhibition by BEL might be attributable to iPLA$_2\gamma$ or other novel isozymes.

In this study, we examined the cellular fatty acid-releasing and prostaglandin (PG)-biosynthesizing functions of iPLA$_2\gamma$ in comparison with those of other intracellular PLA_2 enzymes. Our results indicate that iPLA$_2\gamma$ has the ability to promote basal and stimulus-coupled AA release; that iPLA$_2\gamma$ displays unique cyclooxygenase (COX) coupling for immediate and delayed PGE_2 production; that iPLA$_2\gamma$, iPLA$_2\beta$, and cPLA$_2\alpha$ act on different cellular phospholipid pools; and that the 63-kDa form (relative to the 88-kDa full-length form) of iPLA$_2\gamma$ is dominant in several cell lines and is located in peroxisomes. Furthermore, the elevated expression of iPLA$_2\gamma$ in human colorectal adenocarcinoma implicates its potential role in tumorigenesis.

EXPERIMENTAL PROCEDURES

Materials—Culture of human embryonic kidney HEK293 cells, the human colorectal adenocarcinoma cell lines HCA-7 and WiDr, the human bronchial epithelial cell line BEAS-2B, the rat fibroblastic cell line 3Y1, and the mouse Leydig cell line I-10 was performed in RPMI 1640 medium (Nissui Pharmaceutical Co., Ltd.) containing 10% (v/v) fetal calf serum (FCS) (Bioserum) as described previously (36–40). Goat anti-human COX-1 and anti-human COX-2 antibodies and rabbit anti-human group IVA cPLA$_2\alpha$ antibody were purchased from Santa Cruz Biotechnology, Inc. Mouse anti-FLAG antibody and etoposide were obtained from Sigma. Mouse anti-human PEX19 antibody was obtained from BD Biosciences. iPLA$_2\gamma$, iPLA$_2\beta$, cPLA$_2\alpha$, and cPLA$_2\gamma$ cDNAs were described previously (12, 32, 41). Lipofectamine 2000, Opti-MEM medium, TRIzol reagent, Geneticin, and blasticidin were obtained from Invitrogen. Fluorescein isothiocyanate-, Cy3-, and horseradish peroxidase-conjugated anti-IgG antibodies were purchased from Zymed Laboratories Inc.. Primers for reverse transcription-PCR were from Fasmac. The COX-1 inhibitor valeryl salicylate was a generous gift from Dr. W. Smith (University of Michigan). The COX-2 inhibitor NS-398 and the $iPLA_2$ inhibitor BEL were purchased from Cayman Chemical Co. Other reagents of analytical grade were from Wako Chemicals.

Northern Blotting—Equal amounts (~5 μg) of total RNA obtained from cells using TRIzol reagent were applied to separate lanes of 1.2% (w/v) formaldehyde-agarose gels, electrophoresed, and transferred to Immobilon-N membranes (Millipore). The resulting blots were then probed with appropriate cDNA probes that had been labeled with [^{32}P]dCTP (Amersham Biosciences) by random priming (Takara Biomedicals). Hybridization and subsequent membrane washing were carried out as described previously (12).

Preparation of Anti-iPLA$_2\gamma$ Antibody—Rabbit antiserum against the synthetic peptide RRTTDPKLCITRVEE, which corresponds to residues 371–385 of human iPLA$_2\gamma$ protein, was prepared by Biologica Co. The antiserum was subjected to enzyme immunosorbent assay to determine the antibody titer against the peptide and was used for subsequent analyses. The specificity of the antibody was evaluated by immunoblotting as noted below.

SDS-PAGE and Immunoblotting—Lysates from 10^5 cultured cells were subjected to SDS-PAGE using 7.5 or 10% gels under reducing conditions. The separated proteins were electroblotted onto nitrocellulose membranes (Schleicher & Schüll) with a semidry blotter (Transblot SD system, Bio-Rad). After blocking with 3% (w/v) skim milk in phosphate-buffered saline (PBS) containing 0.05% Tween 20, the membranes were probed with the respective antibodies (1:5000 dilution) for 2 h, followed by incubation with horseradish peroxidase-conjugated anti-goat or anti-rabbit IgG (1:5000 dilution) for 2 h, and then visualized with the ECL Western blot system (PerkinElmer Life Sciences) as described (12).

Immunohistochemistry—Immunohistochemical staining of human tissue sections was performed as described previously (36, 38). Briefly, the tissue sections were incubated with target retrieval solution (Dako Corp.) as required, incubated for 10 min with 3% (v/v) H_2O_2, washed three times with PBS for 5 min each, incubated with 5% (v/v) skim milk for 30 min, washed three times with PBS containing 0.05% Tween 20 for 5 min each, and incubated for 2 h with anti-iPLA$_2\gamma$ antibody at 1:200 dilution in PBS. The sections were then treated with a Catalyzed Signal Amplification system staining kit (Dako Corp.) with diaminobenzidine substrate. The cell type was identified by conventional hematoxylin and eosin staining of serial sections adjacent to the specimen used for immunohistochemistry.

Expression of iPLA$_2\gamma$ by the Lentiviral System—cDNAs for N-terminally FLAG-tagged iPLA$_2\gamma$ and its truncated forms were stably transfected into HEK293 or HCA-7 cells with a ViraPower lentiviral expression system (Invitrogen) according to the manufacturer's instructions. Briefly, cDNAs were amplified by PCR with the Advantage cDNA polymerase mixture (Clontech) and primers 5′-CACCATGGACTACAAGGACGACGATGACAA-3′ (FLAG primer) and 5′-TCACAATTTTGAAAAGAATGGAAG-3′ (iPLA$_2\gamma$-3′ primer) with iPLA$_2\gamma$ cDNA in the pEFBOS-Ffg vector (42) as a template and subcloned into the pLenti6/V4-D-TOPO vector (Invitrogen). The resulting plasmid was transfected into 293FT cells (Invitrogen) with Lipofectamine 2000 in Opti-MEM medium, and aliquots of the supernatants harvested 3 days after transfection were then added to HEK293 or HCA-7 cells. The cells were cultured in the presence of 20–30 μg/ml blasticidin, and the surviving cells that expressed appropriate levels of iPLA$_2\gamma$ were used in subsequent studies.

For construction of N-terminally truncated iPLA$_2\gamma$ cDNAs, PCR was performed with primer 5′-ATGTCCCGTATTAAAAGTACT-3′ (M2), 5′-ATGATTTCACGTTTAGCTCAA-3′ (M3), or 5′-ATGTCTCAACAAAAGGAAAATG-3′ (M4) in combination with the iPLA$_2\gamma$-3′ primer and pEFBOS-Ffg/iPLA$_2\gamma$ as a template. Lentiviruses bearing these truncated iPLA$_2\gamma$ cDNAs as well as those bearing iPLA$_2\beta$, cPLA$_2\alpha$, and cPLA$_2\gamma$ cDNAs were obtained and transfected into HEK293 cells as described above.

Coexpression of PLA$_2$ and COX Enzymes in HEK293 Cells—COX-1 or COX-2 cDNA in the pcDNA3.1/neo(+) vector was transfected into HEK293 cells with Lipofectamine 2000, and Geneticin-resistant clones were selected by limiting dilution and subsequent screening by Western blotting as described previously (43). Each PLA_2 cDNA was then transfected into the COX-1 or COX-2 stable transfectants using the lentiviral system, and the double transfectants were selected by culture with blasticidin, followed by Northern blotting and immunoblotting as described above.

Experiments with iPLA$_2\gamma$ Small Interfering RNA (siRNA)—Two sets of synthetic hairpin-forming oligonucleotides directed to iPLA$_2\gamma$ were prepared (Beck): for set 1 (coding sequences shown in italic type), 5′-GATCCC**G**CTCTTCAGGCTGCA*GTTAG*TTCAAGAGA*CTAACTGCAGCCTGAAGAG*TTTTTTGGAAA-3′ (sense) and 5′-AGCTTTTCCAAAAAA*CTCTTCAGGCTGCAGTTAG*TCTCTTGAA*CTAACTGCAGCCTGAAGAG***C**GG-3′ (antisense); and for set 2, GATCCC**G***TGTGGCAGGCCATTAGAGC*TTCAAGAGA*GCTCTAATGGCCTGCCACA*TTTTTTGGAAA-3′ (sense) and 5′-AGCTTTTCCAAAAAA*TGTGGCAGGCCATTAGAGC*TCTCTTGAA*GCTCTAATGGCCTGCCACA***C**GG-3′ (antisense). After annealing, both sets of double-stranded DNAs harbored BamHI and HindIII sites at each 5′- and 3′-end. After cutting with BamHI and HindIII, they were ligated into the BamHI/HindIII-digested pRNA-U-6.1/Hygro vector (GenScript Corp.) with T4 ligase (Takara Biomedicals). After transformation into Top10 competent cells (Invitrogen), the plasmids were extracted and purified using the Endofree plasmid maxi kit (Qiagen Inc.).

HEK293 cells grown in 12-well plates (Iwaki Glass) were transfected with a mixture of plasmids for iPLA$_2\gamma$ siRNA (sets 1 and 2; 1 μg of each) or 2 μg of mock plasmid (pRNA-U6.1/Hygro) with Lipofectamine 2000 according to the method described previously (44). The cells were then subjected to limiting dilution in culture medium containing 50 μg/ml hygromycin in 96-well plates (Iwaki Glass). The surviving colonies were expanded, and iPLA$_2\gamma$ expression was monitored by immunoblotting.

Measurement of PLA$_2$ Activity—PLA_2 activity was assayed by measuring the amounts of radiolabeled AA or linoleic acid (LA) released from the substrate phosphatidylethanolamine (PE) or phosphatidylcholine (PC) bearing [^{14}C]AA or [^{14}C]LA at the *sn*-2 position (Amersham Biosciences). The substrate in ethanol was dried under a stream of N_2 and dispersed in water by sonication. Each reaction mixture (total volume of 250 μl) consisted of appropriate amounts of the required sample (cell lysate), 100 mM Tris-HCl (pH 7.4), 10 mM EDTA, and 2 μM substrate. After incubation for 30 min at 37 °C, [^{14}C]AA or [^{14}C]LA was extracted by Dole's method (77), and the radioactivity was quantified by liquid scintillation counting as described previously (12).

Assays for AA Release and PGE$_2$ Generation—Cells grown to near confluency in 48-well plates (Iwaki Glass) were incubated overnight with 0.1 μCi/ml [^{3}H]AA or [^{3}H]oleic acid (OA) (Amersham Biosciences). After three washes with fresh medium, 100 μl of culture medium with or without 10 μM A23187 (Calbiochem) or interleukin-1β (IL-1β) (Gen-

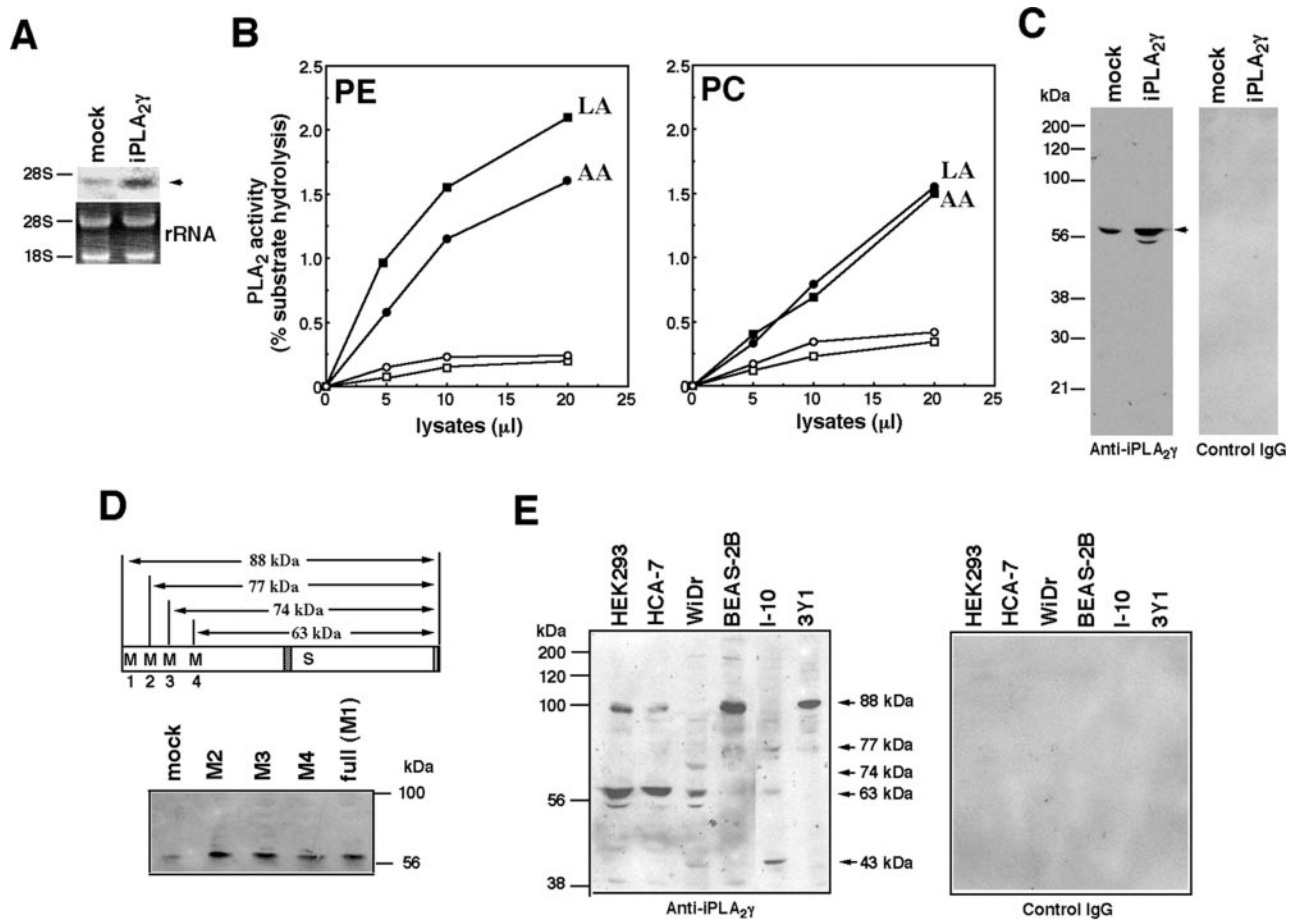

FIG. 1. **Overexpression of iPLA$_2\gamma$ in HEK293 cells.** *A*, iPLA$_2\gamma$ transcripts in mock- or iPLA$_2\gamma$-transfected HEK293 cells were detected by Northern blotting. Equal loading of samples on each lane was verified by rRNA visualized on an agarose gel with ethidium bromide. *B*, iPLA$_2$ activity in cell lysates was measured. 10^7 control cells (□ and ○) and iPLA$_2\gamma$-transfected cells (■ and ●) were lysed by sonication in 1 ml of PBS containing 3 μg/ml leupeptin, 3 μg/ml antipain, and 1 mM phenylmethylsulfonyl fluoride, and aliquots were taken for PLA$_2$ enzyme assay using PE or PC bearing *sn*-2-AA (○ and ●) or *sn*-2-LA (□ and ■) as substrate. *C*, mock- and iPLA$_2\gamma$-transfected cells (10^5 cells/lane) were immunoblotted with anti-iPLA$_2\gamma$ and control antibodies. *D*, HEK293 cells transfected with the full-length (M1) or truncated (M2–M4) iPLA$_2\gamma$ cDNAs (*upper panel*) and control cells were immunoblotted with anti-iPLA$_2\gamma$ antibody (*lower panel*). *E*, various cells (10^5 cells/lane) were immunoblotted with anti-iPLA$_2\gamma$ and control antibodies. Results are representative of three independent experiments.

zyme) was added to each well, and the radioactivities released into the supernatants after incubation for appropriate periods were measured. The percentage release was calculated using the formula $(S/(S + P)) \times 100$, where S and P are the radioactivities measured in the supernatant and cell pellet, respectively, as described previously (12, 43). Aliquots of the supernatants from replicate cells (without preincubation with radiolabeled fatty acids) were subjected to PGE_2 enzyme immunoassay (Cayman Chemical Co.).

Confocal Laser Microscopy—Cells grown in glass-bottomed dishes (Matsunami Glass) precoated with 10 μg/ml fibronectin (Sigma) were fixed with 3% paraformaldehyde for 30 min in PBS. After three washes with PBS, the fixed cells were sequentially treated with 1% (w/v) bovine serum albumin (for blocking) containing 0.5% (w/v) saponin (for permeabilization) in PBS for 1 h, with anti-iPLA$_2\gamma$ antibody (1:200 dilution) in PBS containing 1% albumin for 1 h, and then with fluorescein isothiocyanate-conjugated anti-rabbit IgG (1:200 dilution) in PBS containing 1% albumin for 1 h, with three washes with PBS at each interval. For double immunostaining, cells stained with anti-iPLA$_2\gamma$ antibody were incubated with mouse anti-PEX19 antibody (1:250 dilution) for 2 h, followed by incubation with Cy3-conjugated anti-mouse IgG antibody (1:100 dilution) for 2 h. After six washes with PBS, the fluorescent signal was visualized with an Olympus IX70 laser scanning confocal microscope as described previously (45).

Electrospray Ionization Mass Spectrometry (ESI/MS)—Mass spectra were obtained on a Quattro micro tandem quadrupole mass spectrometer (Micromass) equipped with an electrospray ion source as described previously (46). Lipid extracts from cells were reconstituted in 2:1 chloroform/methanol (100–300 μmol/liter phosphorus), and 2 μl of the sample was injected per run. The samples were introduced using a flow injector into the ESI chamber at a flow rate of 4 μl/min in a solvent system of acetonitrile/methanol/water (2:3:1) containing 0.1% ammonium formate (pH 6.4). The mass spectrometer was operated in the positive and negative scan modes. The flow rate of the nitrogen drying gas was 12 liters/min at 80 °C. The capillary and cone voltages were set at 3.7 kV and 30 V, respectively; argon at $3–4 \times 10^4$ torr was used as the collision gas; and a collision energy of 30–40 V was used for obtaining fragment ions for precursor ions.

RESULTS

Group VIB iPLA$_2\gamma$ Is Expressed Mainly as a 63-kDa Protein in HEK293 Cells—To assess the cellular function of iPLA$_2\gamma$, we used the lentiviral method to transfect HEK293 cells with cDNA for N-terminally FLAG-tagged iPLA$_2\gamma$. As assessed by RNA blotting, endogenous iPLA$_2\gamma$ mRNA was detected faintly in mock-transfected control cells and was increased in iPLA$_2\gamma$-transfected cells (Fig. 1*A*). A lysate of iPLA$_2\gamma$-transfected HEK293 cells showed higher Ca^{2+}-independent PLA$_2$ activity toward pure phospholipid substrates than a lysate of mock-transfected cells (Fig. 1*B*), confirming successful transfection. The lysate of iPLA$_2\gamma$-transfected cells hydrolyzed both PE and PC with a trend to a <2-fold preference for the former, and both *sn*-2-AA and *sn*-2-LA were liberated equally (Fig. 1*B*). Thus, iPLA$_2\gamma$ shows relatively poor selectivity for substrate phospholipids in terms of head group and fatty acid moieties.

To verify further the expression of overexpressed iPLA$_2\gamma$ protein in the transfectants, we performed immunoblotting initially with anti-FLAG antibody. Despite considerable effort,

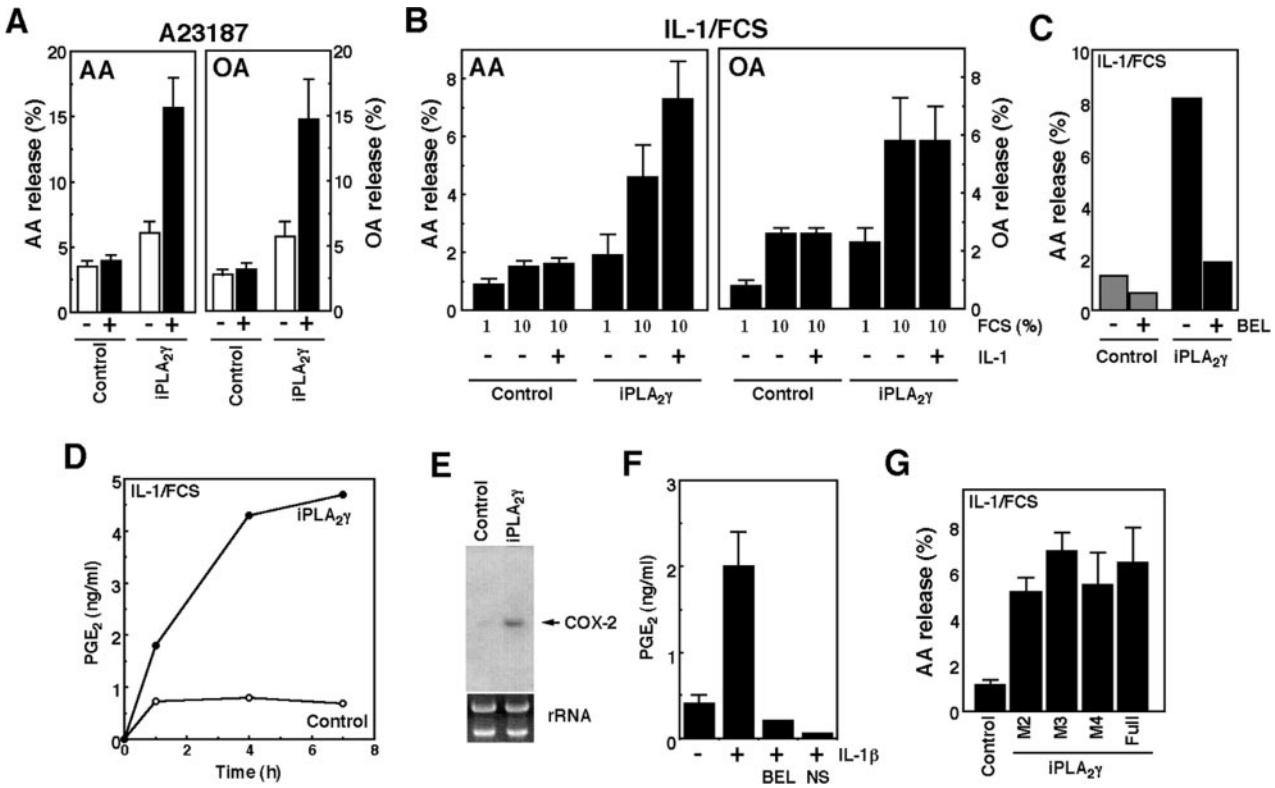

FIG. 2. **Fatty acid release and PGE$_2$ production by iPLA$_2\gamma$-transfected HEK293 cells.** *A* and *B*, control and iPLA$_2\gamma$-transfected cells prelabeled with [^{3}H]AA or [^{3}H]OA were incubated for 30 min with (+) or without (−) 10 μM A23187 in 1% FCS (*A*) or for 4 h with 1 or 10% FCS in the presence (+) or absence (−) of 1 ng/ml IL-1β (*B*) to assess fatty acid release. *C*, [^{3}H]AA-prelabeled cells were preincubated for 2 h with 20 μM BEL and then cultured for 4 h with IL-1/FCS in the continued presence of BEL to assess AA release. *D*, control (○) and iPLA$_2\gamma$-transfected (●) cells were incubated for the indicated time periods with IL-1/FCS, and aliquots of the supernatants were taken for PGE$_2$ enzyme immunoassay. *E*, after incubation for 2 h with IL-1/FCS, control and iPLA$_2\gamma$-transfected cells were subjected to Northern blotting with COX-2 cDNA as a probe. Equal loading of samples on each lane was verified by rRNA visualized on an agarose gel with ethidium bromide. *F*, cells were preincubated for 2 h with 20 μM BEL or 10 ng/ml NS-398 (*NS*) and then cultured for 4 h with IL-1/FCS in the continued presence of each inhibitor to assess PGE$_2$ generation. *G*, cells transfected with full-length iPLA$_2\gamma$ and its truncated forms were assessed for [^{3}H]AA release. The expression levels of the mutant and full-length enzymes (all expressed as a 63-kDa protein) are shown in Fig. 1*D*. Values are means ± S.E. of four independent experiments in *A*, *B*, *F*, and *G*, and representative results of three experiments are shown in *C*–*E*.

however, we failed to detect a corresponding 88-kDa band (the size predicted from the full-length cDNA) in iPLA$_2\gamma$-transfected HEK293 cells (data not shown). We therefore prepared a rabbit antibody against a peptide corresponding to an internal sequence of human iPLA$_2\gamma$ (residues 371–385). Upon immunoblotting with anti-iPLA$_2\gamma$ (but not control) antibody, an ~60-kDa band was detected in control cells, and this band was increased in iPLA$_2\gamma$-transfected cells (Fig. 1*C*).

Gross and co-workers (33) have recently reported that iPLA$_2\gamma$ contains 4 methionine residues acting as translation initiation sites, resulting in 88-, 77-, 74-, and 63-kDa products in Sf9 insect cells. We therefore speculated that the main ~60-kDa band detected in HEK293 cells may correspond to the product initiated at the fourth methionine and thereby would lack the FLAG epitope, which was located prior to the first methionine. To investigate this possibility, we constructed several N-terminally truncated iPLA$_2\gamma$ constructs in which protein translation would start theoretically at the second (M2), third (M3), and fourth (M4) methionine residues, leading to the production of 77-, 74-, and 63-kDa forms. However, when these constructs were lentivirally transfected into HEK293 cells, all resulted in an immunoreactive ~60-kDa product (Fig. 1*D*). On the basis of these observations, we concluded that iPLA$_2\gamma$ exists mainly as a 63-kDa form, which starts at the fourth methionine, in HEK293 cells.

We then investigated whether the 63-kDa form of iPLA$_2\gamma$ is commonly dominant in various cell types or whether there are other cell types in which larger forms (88, 77, or 74 kDa) are dominantly expressed. After longer exposure of the immunoblot membrane to the film, the 88-kDa full-length form, in addition to the main 63-kDa form as noted above, was faintly detected in parental HEK293 cells (Fig. 1*E*). Similarly, the major 63-kDa and minor 88-kDa forms were detected in the human colorectal adenocarcinoma cell line HCA-7 (Fig. 1*E*). In another human colorectal cancer cell line (WiDr), the expression of the 63-kDa form was also dominant (even though less than in HCA-7 cells), and a faint 74-kDa band was additionally detected. In contrast, the 88-kDa full-length form was expressed predominantly in the human bronchial epithelial cell line BEAS-2B and the rat fibroblastic cell line 3Y1 (Fig. 1*E*). Weak expression of the 77- and 63-kDa forms, as well as a 43-kDa species, the origin of which is currently unknown (probably a product of proteolytic degradation or alternative splicing), was detected in the mouse Leydig cell line I-10 (Fig. 1*E*). No significant bands were detected with control antibody under the same immunoblot conditions.

Fatty Acid Release and PGE$_2$ Production in iPLA$_2\gamma$-overexpressing HEK293 Cells—When mock- and iPLA$_2\gamma$-transfected cells were prelabeled with [^{3}H]AA or [^{3}H]OA and then stimulated for 30 min with A23187, there was a parallel increase in [^{3}H]AA or [^{3}H]OA release in iPLA$_2\gamma$-transfected cells compared with control cells (Fig. 2*A*). Likewise, when these cells were cultured with various concentrations of FCS for 4 h, iPLA$_2\gamma$-transfected cells released more [^{3}H]AA or [^{3}H]OA than did control cells in an FCS concentration-dependent manner (Fig. 2*B*). Addition of IL-1β to 10% FCS (IL-1/FCS) further increased

[^{3}H]AA release by iPLA$_2\gamma$-transfected cells, whereas [^{3}H]OA release was not appreciably affected by IL-1β. The increased [^{3}H]AA release observed in iPLA$_2\gamma$-transfected cells after treatment with IL-1/FCS was reversed to the basal level by the iPLA$_2$ inhibitor BEL (Fig. 2*C*). As shown in Fig. 2*D*, iPLA$_2\gamma$-transfected cells produced more PGE$_2$ than did control cells in response to IL-1/FCS. This PGE$_2$-biosynthesizing response depended on endogenous COX-2 because more COX-2 was induced in IL-1/FCS-treated iPLA$_2\gamma$-transfected cells than in control cells (Fig. 2*E*) and because NS-398, a COX-2 inhibitor, blocked this PGE$_2$ generation almost completely (Fig. 2*F*). This PGE$_2$ production was also suppressed by BEL in iPLA$_2\gamma$-transfected cells (Fig. 2*F*). As shown in Fig. 2*G*, cells transfected with the truncated forms of iPLA$_2\gamma$ (M2, M3, and M4) exhibited increased [^{3}H]AA release, which reached a level similar to that observed in cells transfected with the full-length enzyme.

To gain further insight into the functional modes of iPLA$_2\gamma$, we compared AA release and PGE$_2$ production by iPLA$_2\gamma$ (in terms of COX coupling) with those by several other intracellular PLA$_2$ enzymes, including cPLA$_2\alpha$, cPLA$_2\gamma$, and iPLA$_2\beta$. To this end, cells transfected with cPLA$_2\alpha$, cPLA$_2\gamma$, iPLA$_2\beta$, or iPLA$_2\gamma$ were treated with A23187 for 30 min or with IL-1/FCS for 4 h. As shown in Fig. 3*A*, A23187-induced immediate [^{3}H]AA release by iPLA$_2\gamma$ was comparable with that by cPLA$_2\alpha$, whereas that by cPLA$_2\gamma$ and iPLA$_2\beta$ was weak even if significant. Maximal [^{3}H]AA release by iPLA$_2\gamma$ after treatment with IL-1/FCS reached a level comparable with that by cPLA$_2\alpha$, although more [^{3}H]AA was released by iPLA$_2\gamma$ than by cPLA$_2\alpha$ in the absence of IL-1β (Fig. 3*B*). Indeed, iPLA$_2\gamma$-induced [^{3}H]AA release was obvious even at 1% FCS, whereas [^{3}H]AA release by cPLA$_2\alpha$ was minimal at 1% FCS, modestly increased at 10% FCS, and markedly augmented in the presence of IL-1β (Fig. 3*B*). [^{3}H]AA release by iPLA$_2\beta$ increased to a level slightly lower than that by iPLA$_2\gamma$ in the presence of 10% FCS and was not augmented by IL-1β (Fig. 3*B*). The increase in [^{3}H]AA release by cPLA$_2\gamma$ was modest, although significant (Fig. 3*B*). Kinetic experiments further supported these observations in that, at each time point, [^{3}H]AA release by cPLA$_2\alpha$ was markedly increased by IL-1β; iPLA$_2\beta$ increased [^{3}H]AA release independently of IL-1β; and iPLA$_2\gamma$ elicited FCS-dependent [^{3}H]AA release with a modest enhancement by IL-1β (Fig. 3*C*).

To compare the coupling profiles between these four intracellular PLA$_2$ enzymes and the two COX isoforms, the enzymes were coexpressed in HEK293 cells. Appropriate expression of the PLA$_2$ and COX enzymes in individual cotransfectants was verified by RNA blotting or immunoblotting (data not shown). These cells were then stimulated for 30 min with A23187 (Fig. 3*D*) or for 4 h with IL-1/FCS (Fig. 3*E*) to assess immediate and delayed PGE$_2$ generation, respectively. cPLA$_2\alpha$ increased PGE$_2$ synthesis markedly via both COXs after A23187 stimulation (Fig. 3*D*) and via COX-2 in marked preference to COX-1 after IL-1/FCS stimulation (Fig. 3*E*). cPLA$_2\gamma$ increased PGE$_2$ generation only modestly (in line with its weak AA-releasing property; see above), but its coupling selectivity for the two COX isoforms was similar to that of cPLA$_2\alpha$. iPLA$_2\beta$ modestly increased COX-1-dependent PGE$_2$ production after A23187 stimulation (Fig. 3*D*), whereas no appreciable increase in PGE$_2$ occurred after IL-1β stimulation (Fig. 3*E*). These COX-coupling profiles of cPLA$_2\alpha$, cPLA$_2\gamma$, and iPLA$_2\beta$ in HEK293 cells are consistent with our previous reports (41, 43). Remarkably, iPLA$_2\gamma$-mediated PGE$_2$ generation occurred via COX-1 in marked preference to COX-2 after stimulation with A23187 (Fig. 3*D*) and IL-1β (Fig. 3*E*). The amount of PGE$_2$ produced by iPLA$_2\gamma$/COX-1 reached a level comparable with that produced by cPLA$_2\alpha$/COX-2 (Fig. 3*E*). These results reveal an unusual preferential COX-1 coupling of iPLA$_2\gamma$ in both the immediate and delayed responses.

iPLA$_2\gamma$ Promotes Cell Death-associated AA Release—Several previous studies have demonstrated the role of iPLA$_2\beta$ in accelerated membrane hydrolysis in apoptotic cells (18–21). To explore whether or not iPLA$_2\gamma$ exhibits a similar effect, we treated control and iPLA$_2\beta$- or iPLA$_2\gamma$-expressing HEK293 cells with etoposide, a cell death inducer. Etoposide treatment led to a dose-dependent (Fig. 4*A*) and time-dependent (Fig. 4*B*) increase in [^{3}H]AA release in control cells, which was markedly augmented in both iPLA$_2\beta$- and iPLA$_2\gamma$-transfected cells. Although iPLA$_2\beta$ has been shown to be activated by caspase-3-dependent cleavage during apoptosis (18, 20, 21), no such proteolytic cleavage or increased expression of iPLA$_2\gamma$ was observed following etoposide treatment (data not shown), suggesting that cell death is accompanied by membranous changes that lead to increased susceptibility to iPLA$_2\gamma$.

Role of Endogenous iPLA$_2\gamma$ in Cellular AA Release—To assess the contribution of endogenous iPLA$_2\gamma$ to fatty acid release in HEK293 cells, we introduced siRNA for iPLA$_2\gamma$ into these cells to reduce the expression of endogenous iPLA$_2\gamma$. As shown in Fig. 5*A*, expression of endogenous iPLA$_2\gamma$ was markedly reduced in cells transfected with iPLA$_2\gamma$ siRNA. When these cells were prelabeled with [^{3}H]AA and then cultured for 4 h with 10% FCS in the presence or absence of IL-1β, there was an ~50% reduction of [^{3}H]AA release in siRNA-treated cells relative to control cells (Fig. 5*B*). Likewise, etoposide-induced [^{3}H]AA release was significantly reduced in cells treated with iPLA$_2\gamma$ siRNA. These results indicate that endogenous iPLA$_2\gamma$ significantly contributes to basal and cell death-associated AA release in HEK293 cells. Given that the reduction of [^{3}H]AA release by iPLA$_2\gamma$ siRNA was no >50% (Fig. 5, *B* and *C*), despite an ~80% reduction of the iPLA$_2\gamma$ expression level (Fig. 5*A*), other endogenous PLA$_2$ enzymes may also be involved in this event. It is likely that endogenous iPLA$_2\beta$ participates in the residual [^{3}H]AA release in iPLA$_2\gamma$ siRNA-treated cells because it was reduced by ~70% by BEL (data not shown).

Analysis of Endogenous Phospholipids by ESI/MS—Although the above data suggest that iPLA$_2\gamma$ and other intracellular PLA$_2$ enzymes exhibit distinct fatty acid-releasing profiles and hence may act on different phospholipid pools, the release of ^{3}H-labeled fatty acids that had been incorporated into cellular membranes might not necessarily reflect the true dynamics of endogenous lipids. We therefore performed ESI/MS analysis to examine the fatty acid composition of phospholipid molecular species in iPLA$_2\gamma$-, iPLA$_2\beta$-, and cPLA$_2\alpha$-transfected HEK293 cells in comparison with mock-transfected control cells. Representative ESI/MS patterns of PE species extracted from mock-, iPLA$_2\gamma$-, and cPLA$_2\alpha$-transfected cells are shown in Fig. 6.

This analysis revealed that many, if not all, subclasses of PE, including those bearing $C_{18:1}$, $C_{18:2}$, $C_{20:4}$, and $C_{22:6}$ at the *sn*-2 position, were markedly reduced in iPLA$_2\gamma$-transfected cells compared with control cells (Fig. 7*A*, *left panel*). In particular, the decrease in the alkenyl form of PE (plasmalogen) with polyunsaturated fatty acids ($C_{20:4}$ and $C_{22:6}$) was striking. Of the PC subclasses, only the major subclass with *sn*-1-$C_{16:0}$ and *sn*-2-$C_{18:2}$ ($C_{16:0}/C_{18:2}$) was significantly reduced in iPLA$_2\gamma$-transfected cells compared with control cells (Fig. 7*B*, *left panel*). Phosphatidylinositol (PI), which was composed mainly of $C_{18:0}/C_{20:4}$, was also markedly decreased in iPLA$_2\gamma$-transfected cells (Fig. 7*C*, *left panel*).

Comparison between iPLA$_2\beta$-transfected and control cells demonstrated that, in the former cells, PE (Fig. 7*A*, *middle panel*) and PC (Fig. 7*B*, *middle panel*) subclasses with $C_{16:0}$ at

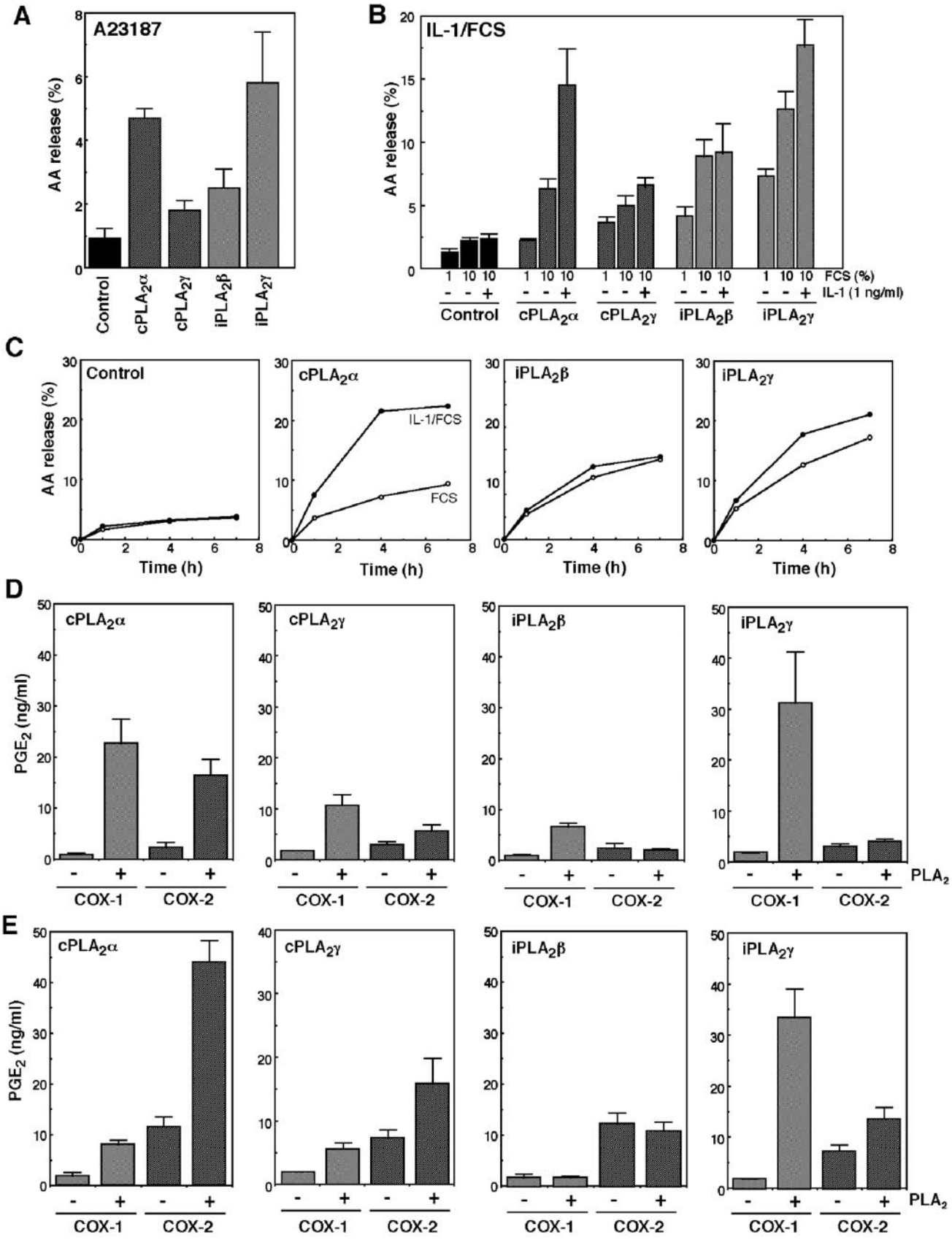

FIG. 3. **Functional coupling between various intracellular PLA$_2$ enzymes and two COXs.** *A* and *B*, control HEK293 cells and cells transfected with cPLA$_2\alpha$, cPLA$_2\gamma$, iPLA$_2\beta$, or iPLA$_2\gamma$ were prelabeled with [^{3}H]AA and then treated for 30 min with 10 μM A23187 in 1% FCS (*A*) or for 4 h with 1 or 10% FCS in the presence (+) or absence (−) of 1 ng/ml IL-1β (*B*) to assess [^{3}H]AA release. *C*, shown is the time course of [^{3}H]AA release from control cells or cells transfected with cPLA$_2\alpha$, iPLA$_2\beta$, or iPLA$_2\gamma$ after treatment for the indicated times periods with 10% FCS alone (○) or IL-1/FCS (●). *D* and *E*, COX-1- or COX-2-expressing HEK293 cells were cotransfected with (+) or without (−) each PLA$_2$. The cells were then stimulated for 30 min with A23187 in 1% FCS (*D*) or for 4 h in IL-1/FCS (*E*) to assess PGE$_2$ generation. Values are means ± S.E. of four independent experiments in *A*, *B*, *D*, and *E*, and a representative result of two reproducible experiments is shown in *C*.

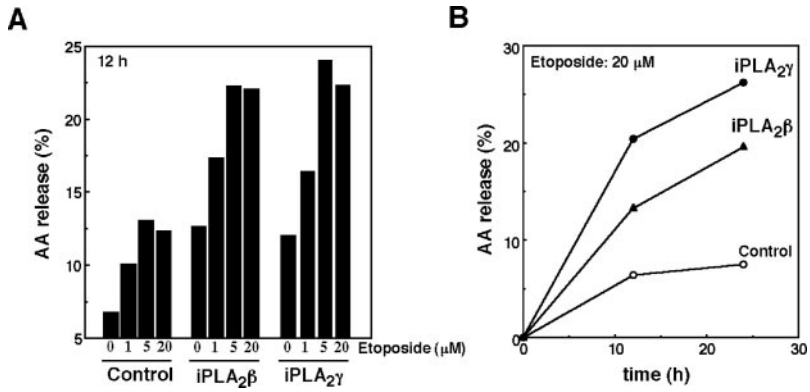

FIG. 4. **Cell death-associated AA release.** [^{3}H]AA-prelabeled control HEK293 cells or cells transfected with iPLA$_2\beta$ or iPLA$_2\gamma$ were treated for 24 h with the indicated concentrations of etoposide (*A*) or for the indicated time periods with 20 μM etoposide (*B*) to assess [^{3}H]AA release. Results are representative of two reproducible experiments.

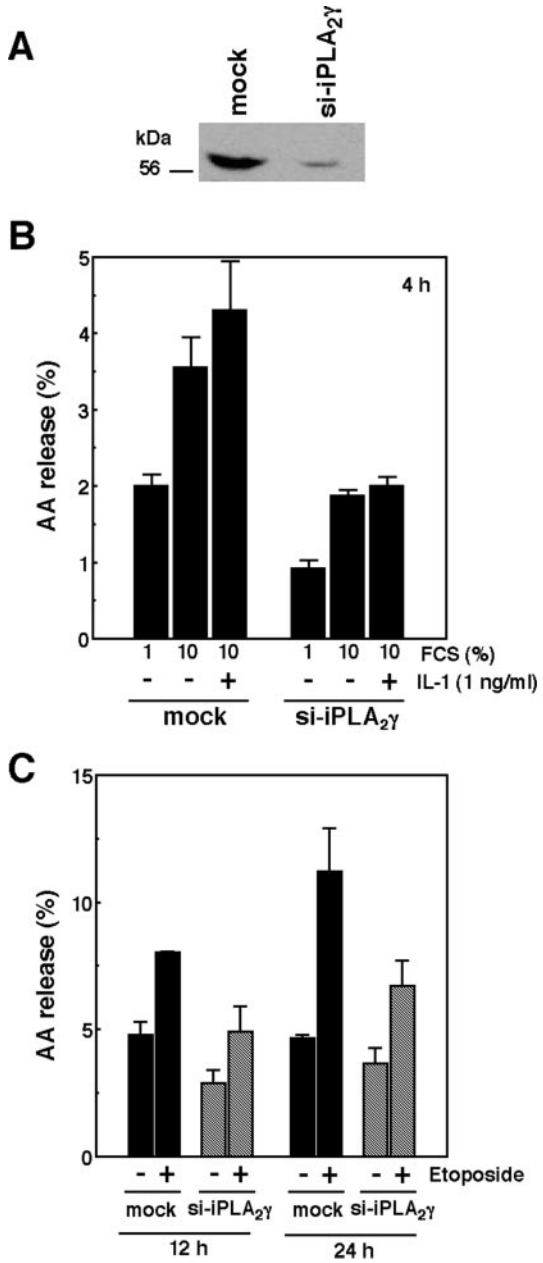

FIG. 5. **Knockdown of iPLA$_2\gamma$ by siRNA.** *A*, HEK293 cells were transfected with a mock or iPLA$_2\gamma$ siRNA (*si-iPLA$_2\gamma$*) plasmid, and 2×10^5 cells were subjected to immunoblotting with anti-iPLA$_2\gamma$ antibody. *B* and *C*, the cells shown in *A* were prelabeled with [^{3}H]AA and then incubated for 4 h with 1 or 10% FCS in the presence (+) or absence (−) of 1 ng/ml IL-1β (*B*) or for 12–24 h in the presence (+) or absence (−) of 10 μM etoposide (*C*) to assess [^{3}H]AA release. Values are means ± S.E. of three independent experiments in *B* and *C*.

the *sn*-1 position were selectively decreased irrespective of *sn*-2-fatty acid moieties. This result suggests that, although iPLA$_2\beta$ does not discriminate *sn*-1/*sn*-2-fatty acids and head groups of substrates *in vitro* (47), it preferentially acts on phospholipids with $C_{16:0}$ at the *sn*-1 position in HEK293 cells, possibly through compartmentalization in the particular membranes enriched in such lipids. Conversely, the contents of PC with $C_{16:0}/C_{16:1}$ (Fig. 7*B*, *middle panel*) and PI with $C_{18:0}/C_{20:4}$ (Fig. 7*C*, *middle panel*) were higher in iPLA$_2\beta$-transfected cells than in control cells, which may be a reflection of phospholipid remodeling.

PE (Fig. 7*A*, *right panel*) and PI (Fig. 7*C*, *right panel*) subclasses with AA at the *sn*-2 position were decreased rather selectively in cPLA$_2\alpha$-transfected cells compared with control cells, consistent with the AA selectivity of this enzyme. Alkyl-PE with $C_{16:0}/C_{18:2}$ and alkenyl-PE with $C_{18:0}/C_{22:6}$ were also significantly reduced in cPLA$_2\alpha$-transfected cells (Fig. 7*A*, *right panel*). Unexpectedly, no appreciable alteration in the fatty acid composition of PC was observed in cPLA$_2\alpha$-transfected cells (Fig. 7*B*, *right panel*), despite the fact that cPLA$_2\alpha$ has been proposed to translocate into PC-rich membranes (48). This result, together with the relatively low content of AA-containing PC (Fig. 7*B*), implies that PC does not represent a major source of the AA released by cPLA$_2\alpha$ in HEK293 cells under the present experimental setting.

iPLA$_2\gamma$ Facilitates Proliferation of Colorectal Cancer Cells—To exclude the possibility that the PGE$_2$-biosynthesizing property of iPLA$_2\gamma$ is peculiar to HEK293 cells, we attempted to transfect iPLA$_2\gamma$ cDNA into several cell types. By following the lentiviral transfection strategy, we obtained two lines of HCA-7 cells overexpressing iPLA$_2\gamma$, which appeared as a 63-kDa form (Fig. 8*A*). As in the case of HEK293 cells (Figs. 2 and 3), these transfectants released, in an FCS-dependent manner, more [^{3}H]AA (Fig. 8*B*) and PGE$_2$ (Fig. 8*C*) than did control cells. Previous studies have shown that HCA-7 cells express both COX-1 and COX-2 constitutively and that the production of PGE$_2$ by these cells occurs predominantly through COX-2 during cell culture (36, 49). Consistent with this, PGE$_2$ production by control cells was inhibited almost completely by NS-398, a COX-2 inhibitor, but not by valeryl salicylate, a COX-1 inhibitor (Fig. 8*D*). Of interest, PGE$_2$ generation by iPLA$_2\gamma$-transfected cells showed partial sensitivity to both COX-1 and COX-2 inhibitors (Fig. 8*D*), suggesting the contribution of both COX isoforms to iPLA$_2\gamma$-mediated PGE$_2$ generation in HCA-7 cells. The expression levels of endogenous cPLA$_2\alpha$, COX-1, COX-2, and microsomal PGE$_2$ synthase-1 were unchanged in HCA-7 cells transfected with iPLA$_2\gamma$ (data not shown).

Because PGE$_2$ is known to promote the proliferation of several colon cancer cells (50), we investigated the impact of iPLA$_2\gamma$ overexpression on the growth of HCA-7 cells, the proliferation of which depends on *de novo* synthesized PGE$_2$ (36, 49). As shown in Fig. 8*E*, the two iPLA$_2\gamma$-transfected cell lines

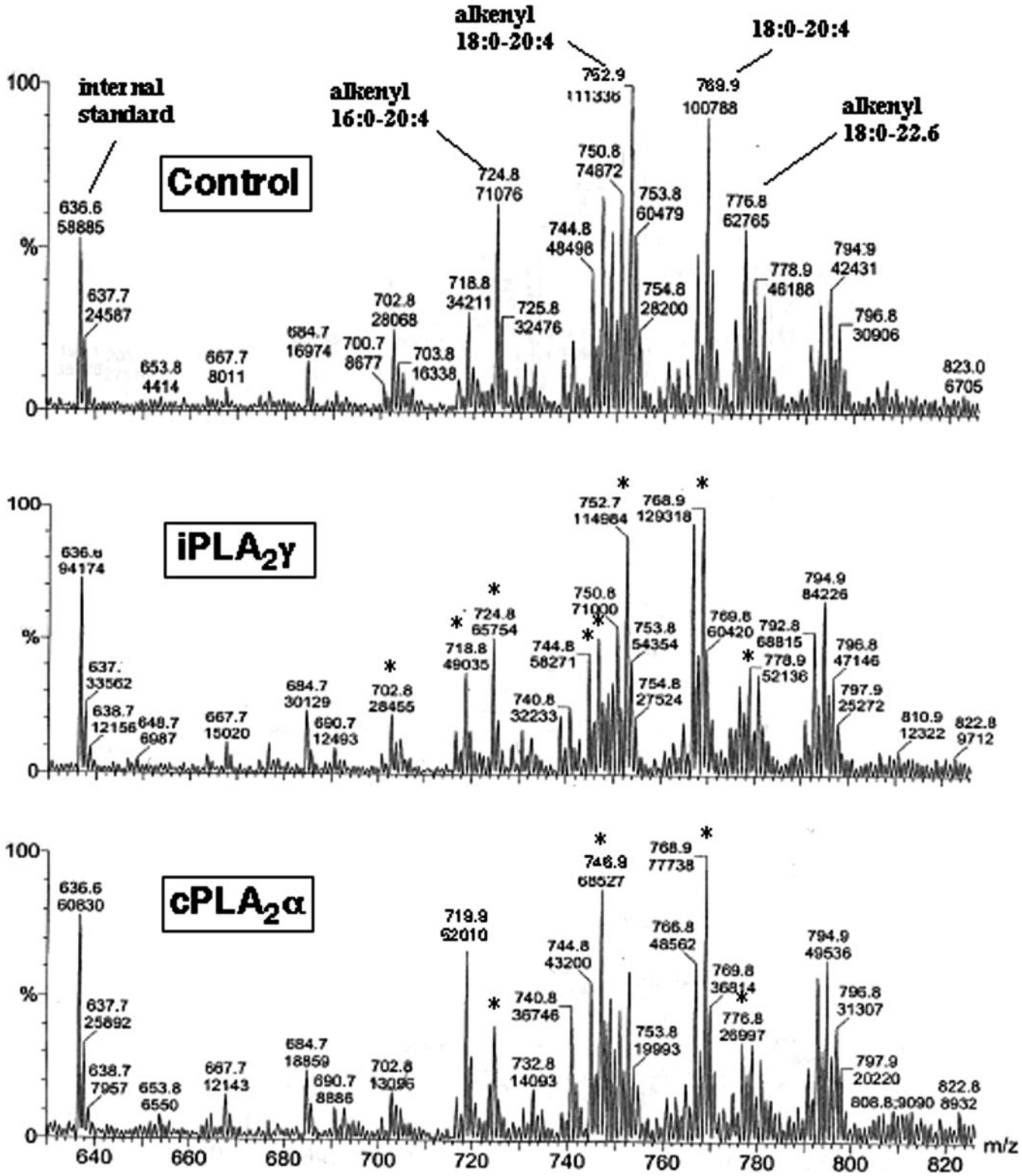

FIG. 6. **ESI/MS analysis of PE species in control and iPLA$_2\gamma$- or cPLA$_2\alpha$-transfected HEK293 cells.** Total lipids were extracted from cells maintained in medium containing 10% FCS and then subjected to lipid ESI/MS analysis. The ESI/MS spectra in the negative ion scan mode are shown. The height of each peak was compared with that of the internal standard (diacyl-PE with $C_{14:0}/C_{14:0}$). *Asterisks* indicate the major peaks that differ between PLA$_2$-transfected and control cells.

grew ~3-fold faster than the control cells in culture with various FCS concentrations (1 and 5%), an event that was correlated with increased PGE_2 synthesis (Fig. 8*C*). Faster growth of iPLA$_2\gamma$-transfected cells compared with control cells was also evident in photographs taken during culture (Fig. 8*F*).

Attempts to achieve iPLA$_2\gamma$ overexpression in BEAS-2B and 3Y1 cells, which endogenously express the 88-kDa form (Fig. 1*E*), by several transfection methods (lipofection and lentivirus- and adenovirus-based methods) were unsuccessful. Although the reason for this technical difficulty is unknown, a possible explanation is that accumulation of full-length iPLA$_2\gamma$ might perturb the membranes of a particular organelle that is important for cell survival (see "Discussion").

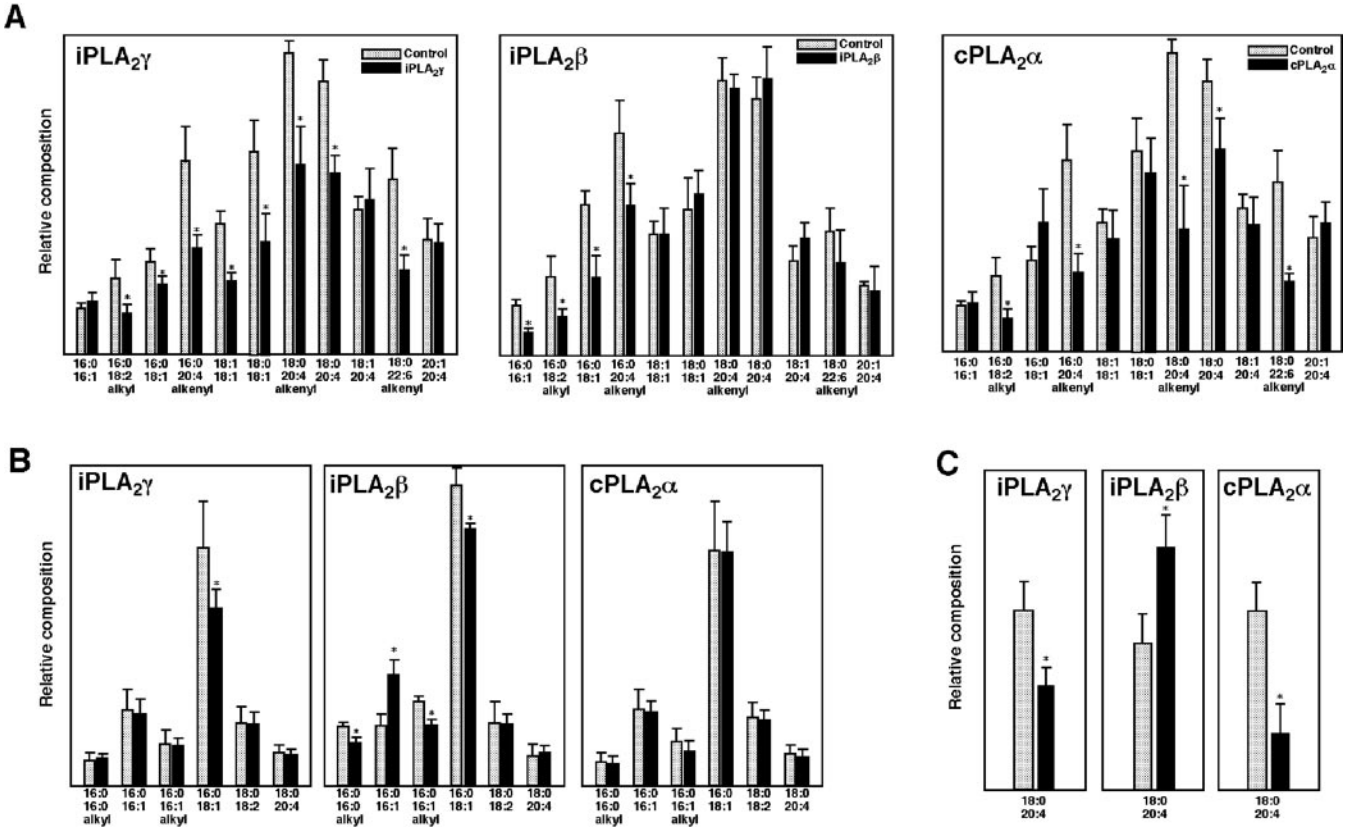

FIG. 7. **Comparison of PE, PC, and PI species between control and PLA$_2$-transfected HEK293 cells.** Shown is a comparison of the relative compositions of PE (*A*), PC (*B*), and PI (*C*) subclasses between control cells (*shaded bars*) and iPLA$_2\gamma$-, iPLA$_2\beta$-, or cPLA$_2\alpha$-transfected cells (*solid bars*). The peak area of each phospholipid subclass in the ESI/MS analysis was calibrated by that of the internal standard. Cells maintained in medium containing 10% FCS were used in this analysis. Values are means ± S.E. of three independent experiments. *, $p < 0.05$ *versus* the respective phospholipids subclass in control cells.

Immunohistochemistry—The finding that iPLA$_2\gamma$ facilitates PGE_2 generation and proliferation of HCA-7 cells (Figs. 7 and 8) prompted us to investigate the expression of this enzyme in human colorectal cancer tissues by immunohistochemistry with anti-iPLA$_2\gamma$ antibody. Intriguingly, positive staining for anti-iPLA$_2\gamma$ antibody was detected in adenocarcinoma cells in four independent human colon cancer tissue sections (Fig. 9, *c–f*). In contrast, iPLA$_2\gamma$ immunoreactivity in glandular cells in sections from normal subjects (Fig. 9, *a* and *b*) and those adjacent to tumor cells (Fig. 9*f*) was scarce. Staining of the submucosal interstitium (in both normal and cancer sections) (Fig. 9, *a–f*) and the lymph aggregates (Fig. 9*f*) was also minimal. Staining of adenocarcinoma tissue with control antibody was negative (Fig. 9*g*). These observations indicate that iPLA$_2\gamma$ expression is elevated in human colorectal adenocarcinoma cells *in vivo*.

Subcellular Localization of iPLA$_2\gamma$—Finally, to assess the subcellular localization of iPLA$_2\gamma$, immunofluorescence confocal microscopy with anti-iPLA$_2\gamma$ antibody was carried out using HEK293 and HCA-7 cells, in which the 63-kDa form of the enzyme is predominantly expressed (see above). In mock-transfected control HEK293 (Fig. 10*A*) and HCA-7 (Fig. 10*B*) cells, faint signals were detected in the cytoplasm with a tendency to form a punctate pattern. These punctate signals were more obvious in cells transfected with iPLA$_2\gamma$ (Fig. 10, *A* and *B*). Because iPLA$_2\gamma$ has a peroxisomal localization signal near the C terminus (31, 32), we performed double immunostaining of these cells with antibodies to iPLA$_2\gamma$ and PEX19, a peroxisomal protein. As shown in Fig. 10*C* (HEK293 cells) and Fig. 10*D* (HCA-7 cells), the punctate signals for iPLA$_2\gamma$ largely overlapped with those for PEX19. Thus, the 63-kDa form of iPLA$_2\gamma$ is distributed mainly in the peroxisomes, as has been recently proposed by Gross and co-workers (33) on the basis of a fractionation study of rat liver homogenates.

DISCUSSION

A large body of experimental evidence (both *in vitro* and *in vivo*) indicates that group IVA cPLA$_2\alpha$, an intracellular Ca^{2+}-dependent enzyme that exhibits AA preference, is a key regulator of the initiation of stimulus-coupled lipid mediator production in a wide variety of mammalian cells (3–10). Although the functions of other cPLA$_2$ isoforms remain elusive, group IVC cPLA$_2\gamma$, the only Ca^{2+}-independent cPLA$_2$ member that is constitutively associated with the endoplasmic reticulum and Golgi membranes, has been recently shown to have the ability to promote eicosanoid production or remodeling of some PE subclasses with polyunsaturated fatty acids when overexpressed in certain cell types (41, 51, 52). Group VIA iPLA$_2\beta$, a cytosolic form of iPLA$_2$, has been implicated in membrane remodeling (11, 12) and eicosanoid generation (13–16), which may be in turn linked to its regulatory roles in secretion (22, 23), vascular relaxation (24), myocardial ischemia (27), cell proliferation and differentiation (17), and apoptosis (18–21). iPLA$_2\beta$ also appears to play an important role in the activation of store-operated channels and capacitative Ca^{2+} influx (26), an event that might be related to the defect in sperm motility (a process in which Ca^{2+} entry is obligatory) in iPLA$_2\beta$-deficient mice (28). In this study, we have extended our understanding of the functional diversity of intracellular PLA$_2$ enzymes by examining the cellular fatty acid-releasing property of group VIB iPLA$_2\gamma$, a novel membrane-associated iPLA$_2$ isoform that was originally identified from a search of a nucleic

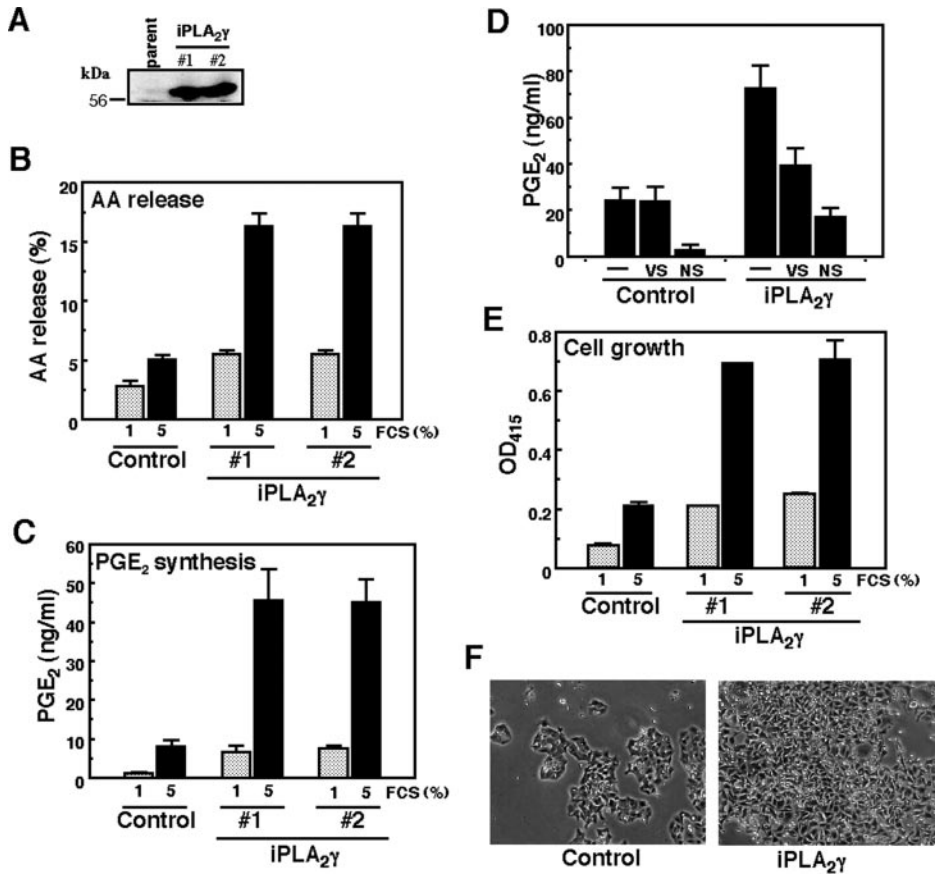

FIG. 8. **Effects of iPLA$_2\gamma$ overexpression on HCA-7 cells.** *A*, mock- or iPLA$_2\gamma$-transfected (two clones) cells were immunoblotted with anti-iPLA$_2\gamma$ antibody. *B*, [^{3}H]AA-prelabeled cells were cultured for 4 h with 1 or 5% FCS to assess [^{3}H]AA release. *C*, the supernatants of replicate cells were taken for PGE$_2$ enzyme immunoassay. *D*, control or iPLA$_2\gamma$-transfected cells were preincubated with the COX-2 inhibitor NS-398 (*NS*; 10 ng/ml) or the COX-1 inhibitor valeryl salicylate (*VS*; 500 μM) for 2 h and then incubated for 4 h with 10% FCS to assess PGE$_2$ generation. *E* and *F*, the growth of control or iPLA$_2\gamma$-transfected cells over 1 week of culture in 5% FCS was evaluated with a cell counting kit (Dojindo) (*E*) and by photography (*F*). For the cell counting kit assay, cells were seeded at 10^4 cells/ml in 96-well plates (100 μl/well); cultured for 1 week; and then incubated for 1 h with a developing reagent, followed by measurement of the absorbance at 415 nm. Replicate cells were cultured in 6-well plates (2 ml/well) for 1 week, and photographs were taken. Values are means ± S.E. of four independent experiments in *B–E*, and representative results are shown in *A* and *F*.

acid data base as a molecule with a region homologous to the catalytic domain of iPLA$_2\beta$ (31, 32).

Our study has revealed the following novel and intriguing aspects of iPLA$_2\gamma$. First, iPLA$_2\gamma$ augments basal, stimulus-coupled, and cell death-associated fatty acid release and shows preferential coupling with COX-1, rather than COX-2, for PGE$_2$ production. Second, iPLA$_2\gamma$ protein is expressed as multiple forms with different sizes in distinct cell types and even in a single cell type, and among these forms, the 63-kDa protein is distributed in the peroxisomes. Third, iPLA$_2\gamma$-mediated phospholipid hydrolysis appears to occur in membranes enriched in PE (the alkenyl species in particular) and PI with polyunsaturated fatty acids. This phospholipid subclass selectivity of iPLA$_2\gamma$ is markedly distinct from that of iPLA$_2\beta$ and cPLA$_2\alpha$, suggesting that, beyond the different enzymatic properties of these enzymes, they may act on different cellular membrane compartments. Finally, iPLA$_2\gamma$ can facilitate AA release and PGE$_2$ production by, and thereby growth of, human colorectal cancer cells in culture. Moreover, immunohistochemistry revealed elevated expression of iPLA$_2\gamma$ in human colorectal adenocarcinoma cells *in vivo*, raising the possibility that this enzyme may participate in tumorigenesis.

Overexpression of PLA$_2$ enzymes, often in combination with COX isoforms, in HEK293 cells is a useful model system to address their potential abilities to promote cellular AA release and its subsequent metabolism to PGE$_2$ (12, 43, 53–56), even though the relevance of this strategy to pathophysiology needs further elucidation, and some caution has to be exercised in interpreting the comparison between the enzymes in the absence of the data to indicate equal expression and proper subcellular localization of each enzyme. Nevertheless, our previous studies using this system have shown that cPLA$_2\alpha$ (12, 43), several secretory PLA$_2$ enzymes (43, 53–56), and cPLA$_2\gamma$ (41) can elicit stimulus-coupled AA release, which is linked to PGE$_2$ production via both COX-1 and COX-2 in the immediate response and via COX-2 in the delayed response, observations that have been supported by other investigators using distinct experimental approaches (51, 52, 57–61). In contrast, in HEK293 cells, iPLA$_2\beta$ promotes stimulus-independent (basal), fatty acid-nonselective release that is poorly (if at all) coupled with COX-dependent PG synthesis (12, 43), which may be a reflection of its membrane remodeling function. iPLA$_2\beta$ also facilitates apoptosis-associated fatty acid release, during which it can be processed by caspase-3 to several truncated, more active forms (18, 20, 21) or can translocate to the nucleus (19). We have shown here that overexpression of iPLA$_2\gamma$ markedly augmented basal (like iPLA$_2\beta$), stimulus-coupled (like cPLA$_2\alpha$) (Fig. 2), and cell death-associated (like iPLA$_2\beta$) (Fig. 4) fatty acid release and that, conversely, down-regulation of endogenous iPLA$_2\gamma$ using the siRNA technique reduced these AA-releasing responses (Fig. 5). The last finding emphasizes that iPLA$_2\gamma$ is intrinsically involved in membrane hydrolysis, probably in the remodeling of peroxisomal membranes in which this enzyme resides (Fig. 10).

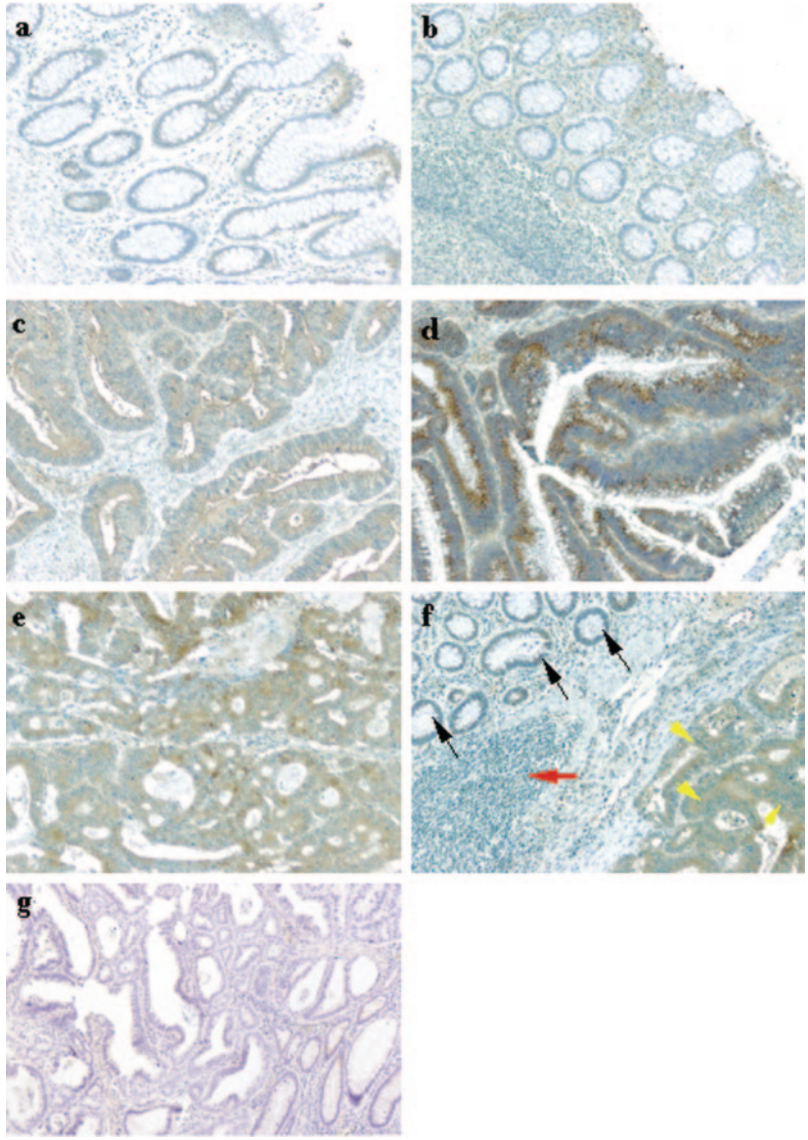

FIG. 9. **Immunohistochemical staining of human colorectal cancer tissues with anti-iPLA$_2\gamma$ antibody.** Tissue sections from two normal subjects (*a* and *b*) and from four patients with colon cancer (*c–f*) were subjected to immunohistochemistry with anti-iPLA$_2\gamma$ antibody. Glandular cells and submucosa in normal tissue sections were largely negative (*a* and *b*). Adenocarcinoma cells stained positively for iPLA$_2\gamma$, whereas the interstitium was negative (*c–f*). Normal glandular cells (*black arrows*) and lymph aggregates (*red arrow*) adjacent to iPLA$_2\gamma$-positive adenocarcinoma cells (*yellow arrowheads*) were not stained appreciably (*f*). Staining of the cancer tissue with control antibody was negative (*g*). Magnification is ×100.

Interestingly, we found that iPLA$_2\gamma$-released AA is preferentially supplied to COX-1 for PGE$_2$ synthesis, an event that is in marked contrast with the fact that cPLA$_2$ and secretory PLA$_2$ enzymes display apparent COX-2 preference (12, 43, 53–56). Indeed, coexpression of iPLA$_2\gamma$ with either COX isoform in HEK293 cells revealed that COX-1-dependent PGE$_2$ production occurred preferentially in A23187-induced immediate and even IL-1/FCS-dependent delayed responses (Fig. 3). In addition, iPLA$_2\gamma$ augmented PGE$_2$ production via both COX-1 and COX-2 in HCA-7 cells (Fig. 8), in which COX-2-mediated PGE$_2$ synthesis dominated unless iPLA$_2\gamma$ was overexpressed. It has been generally believed that COX-2 is favored over COX-1 in cells (particularly when the substrate supply is limited under physiological circumstances), probably because of the higher sensitivity of COX-2 to AA and peroxide compared with COX-1 (43, 62, 63). However, the apparent COX-1 preference of iPLA$_2\gamma$ seems to contradict this belief, indicating that alternative regulatory machinery may account for the preferential iPLA$_2\gamma$/COX-1 coupling. It has been suggested that the spatiotemporal co-localization of eicosanoid-biosynthesizing enzymes can also affect their functional coupling efficiency (64, 65). In this scenario, the distinct subcellular localization of the two COXs, where COX-2 tends to be restricted to the perinuclear membrane and COX-1 to be spread into the cytoplasm along the endoplasmic reticulum membrane (65, 66), might influence their functional coupling with upstream (*i.e.* PLA$_2$ enzymes) and downstream (*i.e.* terminal PG synthases) enzymes, each of which also exhibit specific spatiotemporal subcellular localization. Thus, the AA released by iPLA$_2\gamma$ from the peroxisomal membranes might be more accessible to proximal COX-1 in the endoplasmic reticulum membrane than to distal COX-2 in the perinuclear membrane, a process possibly mediated by certain fatty acid transfer protein(s), by simple diffusion, or by other mechanisms. Although the physiological relevance of the preferential iPLA$_2\gamma$/COX-1 coupling is still obscure, the involvement of COX-1 in prolonged biological processes, such as lung pathogenesis and colon tumorigenesis, has been reported in studies using COX-1 knockout mice (67, 68). It is therefore worthwhile to examine whether iPLA$_2\gamma$ might participate in these pathological events in the context of COX-1 coupling (see below).

As reported previously in insect Sf9 cells (33), iPLA$_2\gamma$ has four potential translation initiation sites, which produce distinct sizes of its protein. Our immunoblot analysis revealed that the 63-kDa form, the translation of which is likely to be initiated at the fourth methionine, was expressed mainly in HEK293, HCA-7, and WiDr cells, whereas the full-size 88-kDa form was dominant in BEAS-2B and 3Y1 cells (Fig. 1). The mechanism underlying cell type-specific control of iPLA$_2\gamma$ translation is unknown at present. As well as this translational

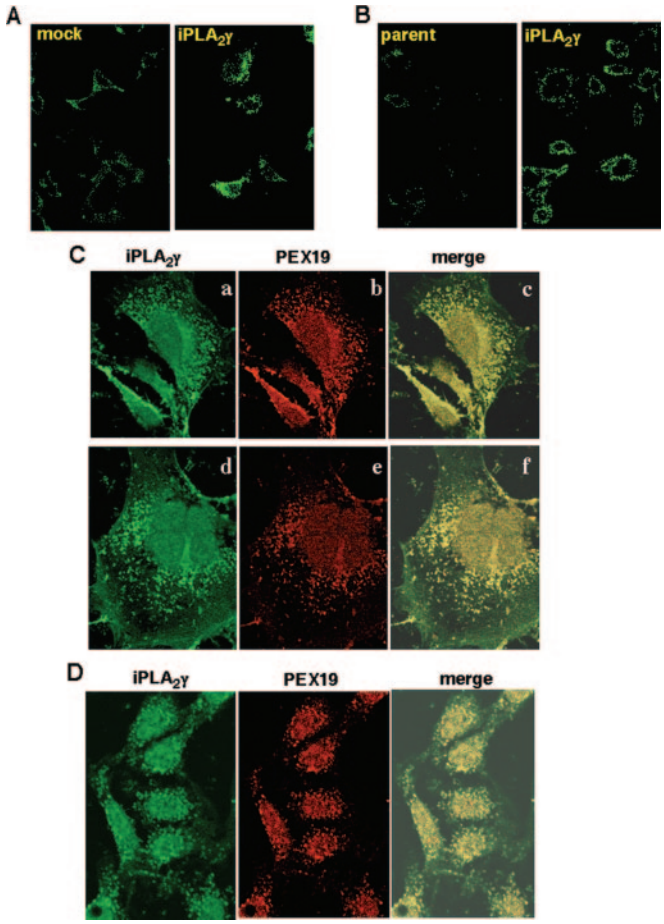

FIG. 10. **Immunofluorescence microscopy.** *A* and *C*, HEK293 cells; *B* and *D*, HCA-7 cells. *A* and *B*, mock- or iPLA$_2\gamma$-transfected cells were stained with anti-iPLA$_2\gamma$ antibody, followed by fluorescein isothiocyanate-conjugated anti-IgG secondary antibody. *C* and *D*, iPLA$_2\gamma$-transfected cells were subjected to double immunostaining with anti-iPLA$_2\gamma$ antibody (*green*) and anti-PEX19 antibody (*red*) in combination with species-matched fluorescein isothiocyanate- and Cy3-conjugated anti-IgG secondary antibodies, respectively. Merged visions (*yellow*) are also shown. Magnifications are ×40 (*A* and *B*), ×200 (*C*, *panels a–c*; and *D*), and ×400 (*C*, *panels d–f*). Control antibody did not provide positive signal (not shown).

regulation, iPLA$_2\gamma$ may undergo post-translational regulation because this enzyme was activated after Ca^{2+} ionophore stimulation (Fig. 2*A*) regardless of its Ca^{2+}-independent catalytic property *in vitro* (Fig. 1*B*) (31, 32). This indicates that the activation of iPLA$_2\gamma$ in agonist-stimulated cells may involve some Ca^{2+}-regulated processes. In support of this speculation, iPLA$_2\gamma$ contains multiple potential phosphorylation sites (32), and our preliminary study showed that the mitogen-activated protein kinase pathway might be involved in the iPLA$_2\gamma$ activation process, probably in an indirect way.[2] It is also notable that the IL-1β-stimulated increase in AA release was not accompanied by an increase in OA release (in contrast to the parallel increase in AA and OA release under basal or A23187-stimulated conditions) in iPLA$_2\gamma$-transfected cells (Fig. 2*B*). This suggests that iPLA$_2\gamma$ may functionally cooperate with cPLA$_2\alpha$ (either directly or indirectly) or that iPLA$_2\gamma$ may act on an AA-rich phospholipid pool in this particular setting.

The ESI/MS analyses demonstrated unexplored and distinct dynamics of the action of intracellular PLA$_2$ enzymes on endogenous phospholipids in HEK293 cells (Figs. 5 and 6), effects that were not previously revealed by study of the release profiles of pre-incorporated ^{3}H-labeled fatty acids. Using a similar ESI/MS approach, Asai *et al.* (52) recently showed that there are increases (rather than decreases) in alkyl-PE with $C_{16:1}/C_{20:4}$ and alkenyl-PE with $C_{18:0}/C_{20:4}$ in cPLA$_2\gamma$-transfected HEK293 cells compared with control cells and thereby proposed an endoplasmic reticulum membrane remodeling function of cPLA$_2\gamma$. Our present study clearly shows that cPLA$_2\alpha$, iPLA$_2\beta$, and iPLA$_2\gamma$ (as well as cPLA$_2\gamma$ (52)) act on different phospholipid subclasses in cellular membrane microenvironments.

In cPLA$_2\alpha$-transfected cells, PE and PI subclasses with polyunsaturated *sn*-2-fatty acids, AA in particular, are reduced rather selectively compared with those in control cells, which agrees with the marked AA selectivity of this enzyme (3, 4). However, no difference in the composition of PC subclasses was observed between cPLA$_2\alpha$-transfected and control cells, indicating that PC, even AA-containing species, is not a major target of cPLA$_2\alpha$ in HEK293 cells under this experimental condition. Although the C2 domain of cPLA$_2\alpha$ has been shown to bind to PC better than to other phospholipids *in vitro* (48, 69), our results suggest that cPLA$_2\alpha$ can obtain access to PE/PI (but not PC)-enriched membrane microdomains in our standard HEK293 cell culture system. Therefore, the recently proposed hypothesis that cPLA$_2\alpha$ translocates to the perinuclear region through recognizing PC-rich membrane in Ca^{2+} ionophore-stimulated HEK293 cells (48) may not be applicable to all situations. Presumably, spatiotemporal production of PI bisphosphate or ceramide 1-phosphate, to which cPLA$_2\alpha$ can bind with high affinity (70, 71), or of other putative cPLA$_2\alpha$-binding proteins (72, 73) might influence the interaction of cPLA$_2\alpha$ with PE/PI-enriched membrane microdomains.

Our results also indicate that iPLA$_2\beta$ and iPLA$_2\gamma$ act on distinct cellular membrane domains, even though both enzymes exhibit similar enzymatic properties in terms of the lack of head group and fatty acid selectivity *in vitro* (31, 32, 47). iPLA$_2\beta$ is distributed in the cytosol, and on which organelle membranes this enzyme actually acts remains controversial. However, our ESI/MS analysis suggests that iPLA$_2\beta$ acts on the particular membrane microdomains enriched in PE and PC with *sn*-1-$C_{16:0}$ irrespective of *sn*-2-fatty acid moieties. In contrast, increases in PC with $C_{16:0}/C_{16:1}$ and PI with $C_{18:0}/C_{20:4}$ in iPLA$_2\beta$-transfected cells relative to those in control cells may indicate that iPLA$_2\beta$-directed membrane hydrolysis is followed by accelerated reacylation by certain acyltransferase(s) or by iPLA$_2\beta$ itself (because it has transacylase activity (74)), resulting in increases in these phospholipid subclasses. In iPLA$_2\gamma$-transfected cells, there are marked decreases in many, if not all, subclasses of PE, including those bearing *sn*-2-$C_{18:1}$, *sn*-2-$C_{18:2}$, *sn*-2-$C_{20:4}$, and *sn*-2-$C_{22:6}$ (alkenyl-PE with AA in particular), as well as in PC with $C_{16:0}/C_{18:0}$ and PI with $C_{18:0}/C_{20:4}$. Given the peroxisomal localization of iPLA$_2\gamma$ (Fig. 10), our results suggest that the peroxisomal membranes in HEK293 cells are enriched in alkenyl-PE bearing AA, which is in close spatial juxtaposition to iPLA$_2\gamma$. This hypothesis is in line with a recent report by Gross and co-workers (33) that rat liver peroxisomal membranes are highly enriched in AA. These facts provide further support for the hypothesis that the peroxisomal membranes represent a potential source of AA for the production of eicosanoids, a process to which iPLA$_2\gamma$ contributes.

Accumulating evidence suggests that COX-2 (75), its downstream enzyme microsomal PGE$_2$ synthase-1 (36), and PGE$_2$ receptors (76) play pivotal roles in the development of gastrointestinal cancer and possibly other cancers. PGE$_2$ promotes the growth and motility of colorectal cancer cells and facilitates angiogenesis (36, 49, 50), a process crucial for the expansion of tumor cells in tissue microenvironments. Notably, the inci-

[2] K. Ueda-Semmyo, Y. Nakatani, H. Sumimoto, M. Murakami, and I. Kudo, unpublished data.

dence of intestinal polyposis has been shown to be ameliorated in COX-1-deficient mice (68). Furthermore, although reduced intestinal polyposis has also been observed in cPLA$_2\alpha$ knockout mice (10), which suggests that cPLA$_2\alpha$ represents an upstream enzyme that supplies AA to COX-2 or COX-1 during colorectal tumorigenesis, this phenotype in these mice is milder than in COX-2-deficient mice (75) or the PGE receptor EP2 (76). These observations have led to the assumption that certain PLA$_2$ enzymes upstream of COX-1 or COX-2, other than cPLA$_2\alpha$, may also take part in the development of gastrointestinal cancer. We have shown here that iPLA$_2\gamma$ has the ability to augment AA release and PGE$_2$ production, which are associated with increased cell growth, in the human colorectal adenocarcinoma cell line HCA-7 (Fig. 8). Moreover, immunohistochemistry of human colorectal cancer tissues revealed that the expression of iPLA$_2\gamma$ was elevated in adenocarcinoma cells from multiple subjects (Fig. 9). These observations raise the intriguing possibility that iPLA$_2\gamma$ may contribute to the development of colorectal cancer in place of or in cooperation with cPLA$_2\alpha$, although confirmation of this hypothesis has to await future studies, including those using iPLA$_2\gamma$ knockout mice.

Questions remain regarding the cellular functions of the larger (including the full-length) forms of iPLA$_2\gamma$ and in which organelles they are located. Because our attempts to overexpress full-length iPLA$_2\gamma$ in several cell lines by multiple transfection protocols were unsuccessful, it may be located in particular organelle(s) where membrane perturbation by overexpression of this enzyme is disadvantageous for cell survival. In this regard, we found recently that the larger forms of iPLA$_2\gamma$ were sorted into the mitochondria.[3] Thus, residence of iPLA$_2\gamma$ in the peroxisomes and mitochondria, which are the sites for fatty acid β-oxidation, implies that this enzyme is associated with organelles with high energy production and consumption. That iPLA$_2\gamma$ mRNA is distributed in tissues with high energy consumption, such as skeletal muscle, heart, and brain (31, 32), is consistent with this notion. It is thus conceivable that, apart from eicosanoid production, one of the functions of iPLA$_2\gamma$ may be related to storage or supply of fatty acids for energy production. Inducible expression of iPLA$_2\gamma$ (as well as several other iPLA$_2$ isozymes) in maturating adipocytes (25, 35) also appears to fit with this concept.

REFERENCES

1. Murakami, M., and Kudo, I. (2001) *Adv. Immunol.* **77,** 163–194
2. Kudo, I., and Murakami, M. (2002) *Prostaglandins Other Lipid Mediat.* **68–69,** 3–58
3. Clark, J. D., Lin, L. L., Kriz, R. W., Ramesha, C. S., Sultzman, L. A., Lin, A. Y., Milona, N., and Knopf, J. L. (1991) *Cell* **65,** 1043–1051
4. Lin, L. L., Wartmann, M., Lin, A. Y., Knopf, J. L., Seth, A., and Davis, R. J. (1993) *Cell* **72,** 269–278
5. Pickard, R. T., Strifler, B. A., Kramer, R. M., and Sharp, J. D. (1999) *J. Biol. Chem.* **274,** 8823–8831
6. Chiba, H., Michibata, H., Wakimoto, K., Seishima, M., Kawasaki, S., Okubo, K., Mitsui, H., Torii, H., and Imai, Y. (2004) *J. Biol. Chem.* **279,** 12890–12897
7. Uozumi, N., Kume, K., Nagase, T., Nakatani, N., Ishii, S., Tashiro, F., Komagata, Y., Maki, K., Ikuta, K., Ouchi, Y., Miyazaki, J., and Shimizu, T. (1997) *Nature* **390,** 618–622
8. Bonventre, J. V., Huang, Z., Taheri, M. R., O'Leary, E., Li, E., Moskowitz, M. A., and Sapirstein, A. (1997) *Nature* **390,** 622–625
9. Nagase, T., Uozumi, N., Ishii, S., Kume, K., Izumi, T., Ouchi, Y., and Shimizu, T. (2000) *Nat. Immunol.* **1,** 42–46
10. Takaku, K., Sonoshita, M., Sasaki, N., Uozumi, N., Doi, Y., Shimizu, T., and Taketo, M. M. (2000) *J. Biol. Chem.* **275,** 34013–34016
11. Balsinde, J., Balboa, M. A., and Dennis, E. A. (1997) *J. Biol. Chem.* **272,** 29317–29321
12. Murakami, M., Shimbara, S., Kambe, T., Kuwata, H., Winstead, M. V., Tischfield, J. A., and Kudo, I. (1998) *J. Biol. Chem.* **273,** 14411–14423
13. Akiba, S., Mizunaga, S., Kume, K., Hayama, M., and Sato, T. (1999) *J. Biol. Chem.* **274,** 19906–19912
14. Jenkins, C. M., Han, X., Mancuso, D. J., and Gross, R. W. (2002) *J. Biol. Chem.* **277,** 32807–32814
15. Yellaturu, C. R., and Rao, G. N. (2003) *J. Biol. Chem.* **278,** 43831–43837
16. Tay, H. K., and Melendez, A. J. (2004) *J. Biol. Chem.* **279,** 22505–22513
17. Roshak, A. K., Capper, E. A., Stevenson, C., Eichman, C., and Marshall, L. A. (2000) *J. Biol. Chem.* **275,** 35692–35698
18. Atsumi, G., Murakami, M., Kojima, K., Hadano, A., Tajima, M., and Kudo, I. (2000) *J. Biol. Chem.* **275,** 18248–18258
19. Shinzawa, K., and Tsujimoto, Y. (2003) *J. Cell Biol.* **163,** 1219–1230
20. Ramanadham, S., Hsu, F. F., Zhang, S., Jin, C., Bohrer, A., Song, H., Bao, S., Ma, Z., and Turk, J. (2004) *Biochemistry* **43,** 918–930
21. Lauber, K., Bohn, E., Krober, S. M., Xiao, Y. J., Blumenthal, S. G., Lindemann, R. K., Marini, P., Wiedig, C., Zobywalski, A., Baksh, S., Xu, Y., Autenrieth, I. B., Schulze-Osthoff, K., Belka, C., Stuhler, G., and Wesselborg, S. (2003) *Cell* **113,** 717–730
22. Balboa, M. A., Saez, Y., and Balsinde, J. (2003) *J. Immunol.* **170,** 5276–5280
23. Ramanadham, S., Hsu, F. F., Bohrer, A., Ma, Z., and Turk, J. (1999) *J. Biol. Chem.* **274,** 13915–13927
24. Seegers, H. C., Gross, R. W., and Boyle, W. A. (2002) *J. Pharmacol. Exp. Ther.* **302,** 918–923
25. Su, X., Mancuso, D. J., Bickel, P. E., Jenkins, C. M., and Gross, R. W. (2004) *J. Biol. Chem.* **279,** 21740–21748
26. Smani, T., Zakharov, S. I., Csutora, P., Leno, E., Trepakova, E. S., and Bolotina, V. M. (2004) *Nat. Cell Biol.* **6,** 113–120
27. Mancuso, D. J., Abendschein, D. R., Jenkins, C. M., Han, X., Saffitz, J. E., Schuessler, R. B., and Gross, R. W. (2003) *J. Biol. Chem.* **278,** 22231–22236
28. Bao, S., Miller, D. J., Ma, Z., Wohltmann, M., Eng, G., Ramanadham, S., Moley, K., and Turk, J. (2004) *J. Biol. Chem.* **279,** 38194–38200
29. Steer, S. A., Wirsig, K. C., Creer, M. H., Ford, D. A., and McHowat, J. (2002) *Am. J. Physiol.* **283,** C1621–C1626
30. Akiba, S., Ohno, S., Chiba, M., Kume, K., Hayama, M., and Sato, T. (2002) *Biochem. Pharmacol.* **63,** 1969–1977
31. Mancuso, D. J., Jenkins, C. M., and Gross, R. W. (2000) *J. Biol. Chem.* **275,** 9937–9945
32. Tanaka, H., Takeya, R., and Sumimoto, H. (2000) *Biochem. Biophys. Res. Commun.* **272,** 320–326
33. Yang, J., Han, X., and Gross, R. W. (2003) *FEBS Lett.* **546,** 247–550
34. van Tienhoven, M., Atkins, J., Li, Y., and Glynn, P. (2002) *J. Biol. Chem.* **277,** 20942–20948
35. Jenkins, C. M., Mancuso, D. J., Yan, W., Sims, H. F., Gibson, B., and Gross, R. W. (2004) *J. Biol. Chem.* **279,** 48968–48975
36. Kamei, D., Murakami, M., Nakatani, Y., Ishikawa, Y., Ishii, T., and Kudo, I. (2003) *J. Biol. Chem.* **278,** 19396–19405
37. Murakami, M., Yoshihara, K., Shimbara, S., Sawada, M., Inagaki, N., Nagai, H., Naito, M., Tsuruo, T., Moon, T. C., Chang, H. W., and Kudo, I. (2002) *Eur. J. Biochem.* **269,** 2698–2707
38. Murakami, M., Nakashima, K., Kamei, K., Masuda, S., Ishikawa, Y., Ishii, T., Ohmiya, Y., Watanabe, K., and Kudo, I. (2003) *J. Biol. Chem.* **278,** 37937–37947
39. Kuwata, H., Nakatani, Y., Murakami, M., and Kudo, I. (1998) *J. Biol. Chem.* **273,** 1733–1740
40. Masuda, S., Murakami, M., Matsumoto, S., Eguchi, N., Urade, Y., Lambeau, G., Gelb, M. H., Ishikawa, Y., Ishii, T., and Kudo, I. (2004) *Biochim. Biophys. Acta* **1686,** 15–23
41. Murakami, M., Masuda, S., and Kudo, I. (2003) *Biochem. J.* **372,** 695–702
42. Tanaka, H., Minakami, R., Kanaya, H., and Sumimoto, H. (2004) *Biochem. Biophys. Res. Commun.* **320,** 1284–1290
43. Murakami, M., Kambe, T., Shimbara, S., and Kudo, I. (1999) *J. Biol. Chem.* **274,** 3103–3115
44. Kamei, D., Yamakawa, K., Takegoshi, Y., Mikami-Nakanishi, M., Nakatani, Y., Oh-Ishi, S., Yasui, H., Azuma, Y., Hirasawa, N., Ohuchi, K., Kawaguchi, H., Ishikawa, Y., Ishii, T., Uematsu, S., Akira, S., Murakami, M., and Kudo, I. (2004) *J. Biol. Chem.* **279,** 33684–33695
45. Murakami, M., Kambe, T., Shimbara, S., Yamamoto, S., Kuwata, H., and Kudo, I. (1999) *J. Biol. Chem.* **274,** 29927–29936
46. Tanaka, M., Kishi, Y., Takanezawa, Y., Kakehi, Y., Aoki, J., and Arai, H. (2004) *FEBS Lett.* **571,** 197–204
47. Tang, J., Kriz, R. W., Wolfman, N., Shaffer, M., Seehra, J., and Jones, S. S. (1997) *J. Biol. Chem.* **272,** 8567–8575
48. Stahelin, R. V., Rafter, J. D., Das, S., and Cho, W. (2003) *J. Biol. Chem.* **278,** 12452–12460
49. Williams, C. S., Watson, A. J., Sheng, H., Helou, R., Shao, J., and DuBois, R. N. (2000) *Cancer Res.* **60,** 6045–6051
50. Marnett, L. J., and DuBois, R. N. (2002) *Annu. Rev. Pharmacol. Toxicol.* **42,** 55–80
51. Stewart, A., Ghosh, M., Spencer, D. M., and Leslie, C. C. (2002) *J. Biol. Chem.* **277,** 29526–29536
52. Asai, K., Hirabayashi, T., Uozumi, N., Houjou, T., Taguchi, R., and Shimizu, T. (2003) *J. Biol. Chem.* **278,** 8809–8814
53. Murakami, M., Kambe, T., Shimbara, S., Higashino, K., Hanasaki, K., Arita, H., Horiguchi, M., Arita, M., Arai, H., Inoue, K., and Kudo, I. (1999) *J. Biol. Chem.* **274,** 31435–31444
54. Murakami, M., Koduri, R. S., Enomoto, A., Shimbara, S., Seki, M., Yoshihara, K., Singer, A., Valentin, E., Ghomashchi, F., Lambeau, G., Gelb, M. H., and Kudo, I. (2001) *J. Biol. Chem.* **276,** 10083–10096
55. Murakami, M., Yoshihara, K., Shimbara, S., Lambeau, G., Gelb, M. H., Singer, A. G., Awada, M., Inagaki, N., Nagai, H., Ishihara, M., Ishikawa, Y., Ishii, T., and Kudo, I. (2002) *J. Biol. Chem.* **277,** 19145–19155
56. Murakami, M., Masuda, S., Shimbara, S., Bezzine, S., Ladzunski, M., Lambeau, G., Gelb, M. H., Matsukura, S., Kokubu, F., Adachi, M., and Kudo, I. (2003) *J. Biol. Chem.* **278,** 10657–10667
57. Kim, Y. J., Kim, K. P., Rhee, H. J., Das, S., Rafter, J. D., Oh, Y. S., and Cho, W. (2002) *J. Biol. Chem.* **277,** 9358–9365
58. Balsinde, J., Balboa, M. A., and Dennis, E. A. (1998) *Proc. Natl. Acad. Sci. U. S. A.* **95,** 7951–7956
59. Hanasaki, K., Ono, T., Saiga, A., Morioka, Y., Ikeda, M., Kawamoto, K.,

[3] H. Sumimoto, unpublished data.

Higashino, K., Nakano, K., Yamada, K., Ishizaki, J., and Arita, H. (1999) *J. Biol. Chem.* **274,** 34203–34211
60. Bezzine, S., Koduri, R. S., Valentin, E., Murakami, M., Kudo, I., Ghomashchi, F., Sadilek, M., Lambeau, G., and Gelb, M. H. (2000) *J. Biol. Chem.* **275,** 3179–3191
61. Satake, Y., Diaz, B. L., Balestrieri, B., Lam, B. K., Kanaoka, Y., Grusby, M. J., and Arm, J. P. (2004) *J. Biol. Chem.* **279,** 16488–16494
62. Bambai, B., Rogge, C. E., Stec, B., and Kulmacz, R. J. (2004) *J. Biol. Chem.* **279,** 4084–4092
63. Wu, G., Kulmacz, R. J., and Tsai, A. L. (2003) *Biochemistry* **42,** 13772–13777
64. Murakami, M., Naraba, H., Tanioka, T., Semmyo, N., Nakatani, Y., Kojima, F., Ikeda, T., Fueki, M., Ueno, A., Oh-Ishi, S., and Kudo, I. (2000) *J. Biol. Chem.* **275,** 32783–32792
65. Ueno, N., Murakami, M., Tanioka, T., Fujimori, K., Urade, Y., and Kudo, I. (2001) *J. Biol. Chem.* **276,** 34918–34927
66. Morita, I., Schindler, M., Regier, M. K., Otto, J. C., Hori, T., DeWitt, D. L., and Smith, W. L. (1995) *J. Biol. Chem.* **270,** 10902–10908
67. Carey, M. A., Germolec, D. R., Bradbury, J. A., Gooch, R. A., Moorman, M. P., Flake, G. P., Langenbach, R., and Zeldin, D. C. (2003) *Am. J. Respir. Crit. Care Med.* **167,** 1509–1515
68. Chulada, P. C., Thompson, M. B., Mahler, J. F., Doyle, C. M., Gaul, B. W., Lee, C., Tiano, H. F., Morham, S. G., Smithies, O., and Langenbach, R. (2000) *Cancer Res.* **60,** 4705–4708
69. Nalefski, E. A., McDonagh, T., Somers, W., Seehra, J., Falke, J. J., and Clark, J. D. (1998) *J. Biol. Chem.* **273,** 1365–1372
70. Das, S., and Cho, W. (2002) *J. Biol. Chem.* **277,** 23838–23846
71. Pettus, B. J., Bielawska, A., Subramanian, P., Wijesinghe, D. S., Maceyka, M., Leslie, C. C., Evans, J. H., Freiberg, J., Roddy, P., Hannun, Y. A., and Chalfant, C. E. (2004) *J. Biol. Chem.* **279,** 11320–11326
72. Nakatani, Y., Tanioka, Y., Sunaga, S., Murakami, M., and Kudo, I. (2000) *J. Biol. Chem.* **275,** 1161–1168
73. Sheridan, A. M., Force, T., Yoon, H. J., O'Leary, E., Choukroun, G., Taheri, M. R., and Bonventre, J. V. (2001) *Mol. Cell. Biol.* **21,** 4470–4481
74. Lio, Y. C., and Dennis, E. A. (1998) *Biochim. Biophys. Acta* **1392,** 320–332
75. Oshima, M., Dinchuk, J. E., Kargman, S. L., Oshima, H., Hancock, B., Kwong, E., Trzaskos, J. M., Evans, J. F., and Taketo, M. M. (1996) *Cell* **87,** 803–809
76. Sonoshita, M., Takaku, K., Sasaki, N., Sugimoto, Y., Ushikubi, F., Narumiya, S., Oshima, M., and Taketo, M. M. (2001) *Nat. Med.* **7,** 1048–1051
77. Dole, V. P., and Meinertz, H. (1960) *J. Biol. Chem.* **235,** 2595–2599